59 p.

UNPUBLISHED PRELIMINARY DATA

SEMIANNUAL STATUS REPORT NO. 3

PROJECT NO. A-635

HEAT TRANSFER TO A GAS CONTAINING A CLOUD OF PARTICLES

Andrew McAlister, Henderson C. Ward, Alberto F. Hidalgo, and Clyde Orr, Jr.

Prepared for
National Aeronautics and Space Adminsitration
Washington, D.C. 20005

Covering the Period
1 June 1963 to 30 November 1963
Printed 10 January 1964

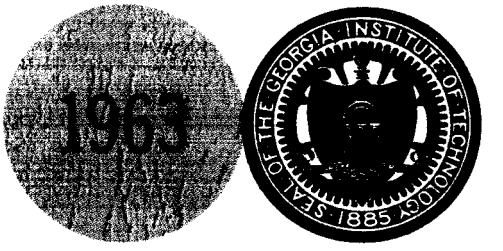

Research Grant NsG-273-62

Engineering Experiment Station
GEORGIA INSTITUTE OF TECHNOLOGY
Atlanta, Georgia

② Engineering Experiment Station

GEORGIA INSTITUTE OF TECHNOLOGY
Engineering Experiment Station
Atlanta, Georgia

1042472

SEMIANNUAL STATUS REPORT NO. 3,

PROJECT NO. A-635

1. HEAT TRANSFER TO A GAS CONTAINING A CLOUD OF PARTICLES

1 Jun. - 30 Nov. 1963

ANDREW MCALISTER, HENDERSON C. WARD,
ALBERTO F. HIDALGO, and CLYDE ORR, JR.

10 Jan. 1964 59p refs

Covering the Period
1 June 1963 to 30 November 1963
Printed 10 January 1964

[2]

(NASA RESEARCH GRANT NsG-273-62)

☐ OTS

(NASA CR-55518) OTS: $5.60 ph, $1.97 mf

Prepared for
NATIONAL AERONAUTICS AND SPACE ADMINISTRATION
WASHINGTON, D.C. 20005

TABLE OF CONTENTS

This report contains 54 pages.

LIST OF FIGURES

LIST OF TABLES

I. SUMMARY

Clouds of particles in a gas increase the ability of the system to absorb radiant energy. The process is difficult to describe quantitatively and there exists an urgent need for engineering data. The objective of this project, therefore, is to provide basic information from both theoretical analyses and experimental observations.

An apparatus was constructed to investigate experimentally the absorptive properties of particle matter suspended in a flowing solid-gas system. As nearly as possible, heat transfer to the solid-gas system and its enclosing conduit was restricted to radiation only. There was, nevertheless, some convective and conductive heat transfer involving the particles, the suspending gas and the quartz conduit. The procedure employed was to generate an aerosol at a constant rate, expose it to a radiant field, and then to determine the heat absorbed by it from an enthalpy balance on the system before and after exposure. The energy gained by the solid-gas system from the glass conduit carrying it was accounted for by determining the amount of heat generated when only air was flowing and subtracting this quantity from the result when particles were in the stream.

Preliminary measurements were made on zinc powder aerosols since zinc was used in developing the apparatus and in establishing experimental procedures. The powder consisted of spherical particles in sizes ranging from submicron to 10 microns in diameter with a mean diameter of 5 microns. This material, being a metal, had a low absorptance and was useful in testing the operational capability of

the apparatus with low absorbing materials. The small particle sizes it contained were also valuable in developing the bag filter employed in the powder recirculation system. Experimental data were collected for powder flow rates of 0.13, 0.19, and 0.25 lb/min. The air flow rate in each case was 3.22 CFM at 1 atm and 70° F. For these conditions 1.6, 2.4, and 2.7 Btu/min, respectively, were absorbed by the solid-gas system. Radiation exposure occurred in a 12.5 inch length of quartz conduit 0.512 inch in diameter. The energy source was at 2160° F ± 10° F, and the radiation from it had to pass through one quartz wall 1.5 millimeter thick and two walls 1.0 millimeter thick to reach the aerosol.

Subsequent to the experiments with zinc powder ferrous sulfide was studied. Three powders were prepared in U.S. standard sieve sizes of 30 to 44, 44 to 53, and 53 to 88 microns. Experiments with conditions the same as for the zinc were performed except that the powder flow rates were 0.059, 0.089, 0.16, and 0.24 lb/min. The 44 to 53 and the 53 to 88 micron fractions had absorptances linear with powder flow rate and at 0.24 lb/min. absorbed 4.8 and 3.5 Btu/min., respectively. For the 30 to 44 micron fraction, the relationship was linear and energy absorptions of 3.0, 4.5, 7.7, and 10.9 Btu/min. were found for the successively increasing powder flow rates. The results appear to be valid within ± 0.5 Btu/min. Work is being continued to obtain data for still smaller particle size fractions.

For the particle-cloud absorption measurement to be generalized by theoretical arguments it was necessary to determine the radiant heat

flux in the aerosol quartz conduit. A device which consisted of a shielded and an exposed thermocouple was constructed for this purpose. The procedure was to expose a thermocouple bead to the radiation within the quartz tube, and to calculate the energy absorbed from a knowledge of its temperature, the convective heat transfer coefficient to the surrounding air, and the temperature of the free stream. From this quantity, the view factors between the bead and the furnace walls, and the emissive properties of the two, the intensity of the radiant field impinging on the thermocouple can be calculated. This phase of the work is still in progress.

Two major results are expected to be derived from the present developments. One is the prediction and experimental verification of the absorptivity of a particle cloud and the second is the description of the rate of heat dissipation and the associated surrounding temperature profiles for particles being heated by radiation. With respect to the former objective, a theoretical development is in progress to evaluate the absorptive power of a cylindrical particle as a function of its size, permeability to radiation, and its length-to-diameter ratio. This approach was taken to account for particle size and irregularity in shape. By numerical methods theoretical results are to be computed taking into account the distributions of particle sizes and length-to-diameter ratios. The results are to be compared with the experimental determinations. It is anticipated that the results obtained in this work can be shown to be valid for any situation where the particle diameter-to-radiation wave length is larger than one.

Heat transfer between suspended particles and the surrounding air was assumed to take place by the particles first gaining heat by isotropic radiation and then dissipating it by conduction to the air. Results for this calculation were presented in Semiannual Status Report No. 2. These data, however, are not directly applicable to the experimental system because an appreciable fraction of the energy transferred to the solid-gas system occurs by convection from the wall of the confining tube which also is heated by radiation. Consequently, this analysis is being extended to apply to the actual case.

II. INTRODUCTION

Clouds of particles suspended in a gas increase the ability of the system to absorb radiant energy. The process is difficult to describe quantitatively because of its strong dependence on the geometry of the system, the temperature and quality of the radiation source, and, most complex of all, the intricate mechanisms of particle absorption, reflection, and scattering of electromagnetic energy. Nevertheless, there exists an urgent need for engineering data describing the process so that practical use may be made of the phenomena. It is the objective of this project, therefore, to provide basic information derived from both theoretical analyses and experimental observations.

This report presents a summary and discussion of the experimental investigation of heat transfer to several zinc-air and ferrous sulfide-air systems. The present status of the theoretical analysis is discussed and areas to be investigated are outlined.

III. EXPERIMENTAL INVESTIGATION

A. Equipment and Procedures

An apparatus was constructed to investigate experimentally the absorptive properties of particle matter suspended in a flowing solid-gas system. It was designed (1) to expose an aerosol, well characterized as to particle shape, particle size, surface area, and concentration to a radiant field in which convection and conduction heat effects, except between the particles and the air, are reduced to a minimum and, (2) to measure the energy absorbed. Exposure to a radiant field occurs in a quartz tube through which the solid-gas systems flow. The quartz conduit is protected from extraneous heat effects other than radiation by its enclosure in an evacuated air space, the outer surface of which is air-cooled. The particle cloud is generated at a constant rate and preconditioned to a steady, known temperature. Then, after passing through the radiant field, the cloud is cooled calorimetrically to determine the heat absorbed. A filter mechanism removes the suspended particles from the air and returns them to the aerosol generator for reuse.

Reference may be made to Semiannual Status Report No. 2 for a detailed description of the apparatus. A schematic representation, however, is given in Figure 1 to show the location of thermocouples and other pertinent information as needed in presenting experimental data.

B. Materials for Study

1. Selection

Preliminary measurements were made on zinc powder aerosols since this material was used in developing the apparatus and in establishing

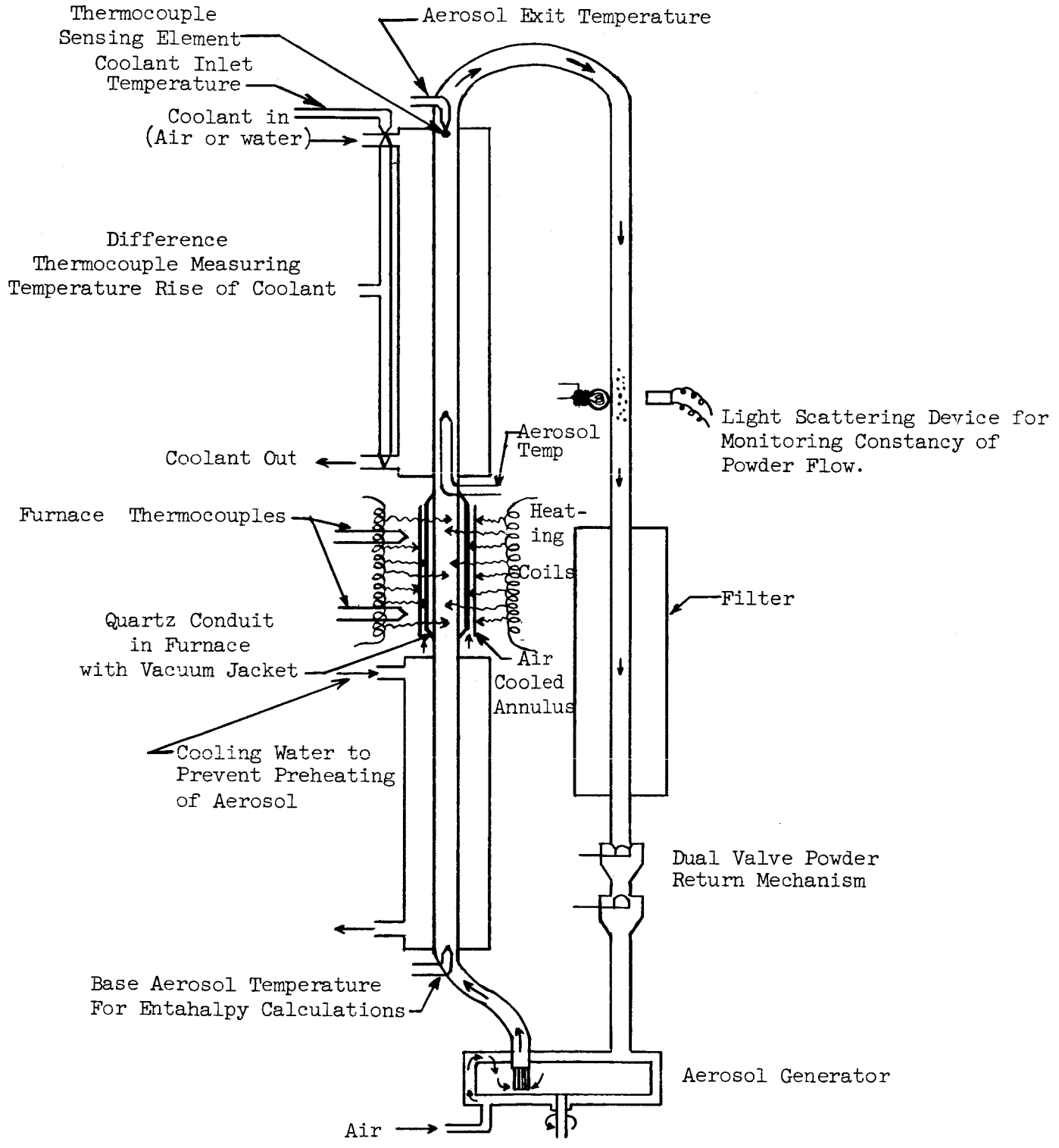

Figure 1. Diagramatic Representation of Heat Transfer Apparatus

experimental procedures. This material, being a metal, has a low absorptivity, which afforded an operational test of the apparatus with low absorbing powders. Also, the zinc powder had an average particle diameter of 5 microns and was useful in testing the bag filter with small particles.

Subsequent to the experiments with zinc powder, ferrous sulfide was selected for study. This material was chosen because of its high absorptivity (opposite to that of zinc), noncorrosive nature, and its availability in lump form which could be subdivided into various size ranges. Also, ferrous sulfide is an electrical nonconductor and hence should have a significant absorption thickness, which is a highly important parameter in the absorption of radiation by particle matter. This material is to be the first of a series of substances possessing varying absorption thicknesses.

2. Preparation

The zinc powder employed was a paint pigment obtained from the Decatur Chemical Company, Decatur, Georgia. This material was used as received since it was for preliminary testing only. Its particle diameter ranged from submicron to a maximum of 10 microns with an average of about 5 microns. The particles were spherical and had a specific surface area of 0.27 m^2/gm as measured by low-temperature nitrogen adsorption.

Ferrous sulfide, the more recent material studied, was lump form, technical grade, from the Baker Chemical Company, Phillipsburg, New Jersey. Preparation of it was initiated by reducing the lumps

to minus 144 U.S. standard sieve size with a mortar and pestle. The product was then ball-milled for one hour intervals and screened until all was less than the 88 micron screen size. Thereafter, standard sieving was continued to yield 88 to 53, 53 to 44, and less than 44 micron fractions. Special screens were then employed to separate the less than 44 micron material into 44 to 30, 30 to 20 and less than 20 micron screen size fractions.

Separation of the less than 20 micron size material is currently in progress. Attempts made to continue the sieving with a 10 micron screen met with little success due to frequent plugging of the sieve. It was found, however, that an additional fraction less than 20 microns could be obtained by sieving with silk cloth. The particles of approximately 10 microns and less adhere to the silk threads while the larger ones pass through. The process here takes advantage of the triboelectric interaction between the ferrous sulfide and the silk threads. Size distributions of less than 10 microns are to be produced by successive ball-milling and silk-screening.

3. Properties of the Ferrous Sulfide Powders

After preparation of the differently sized fractions of ferrous sulfide powders, measurements of their size, surface area and geometrical configuration were made, since these parameters are thought to be significant in establishing the absorptive properties of the powders. The basic measurements involved statistical determinations of the particle geometry, and a low-temperature, nitrogen absorption determination of the specific surface area. A minimum and a maximum

diameter were measured so as to approximate a cylinder since the particles were irregular. It is anticipated that the irregularity of the particles can be accounted for by basing the calculations on cylinders with varying lenth-to-diameter ratios. Figure 2 shows the measurements for a typical set of particles. Note from the figure that $d_{(mean)}$ can sometimes by larger than $d_{(max.)}$. The depth of the particles was assumed to be the same as the minimum visible dimension.

Physical measurements were made both before and after the powders were used in the heat transfer experiments to determine the extent of changes. As expected, significant size and shape differences were found. The results are presented in Table I and in Figures 3 through 5.

TABLE I

NITROGEN ADSORPTION SURFACE AREAS OF POWDERED MATERIALS INVESTIGATED

Material	Surface Area, m^2/gm Before Use	After Use
Zinc	---	0.27
Ferrous Sulfide:		
1. 53 - 88μ Fraction	0.37	0.13
2. 44 - 53μ Fraction	0.35	0.14
3. 30 - 44μ Fraction	--	0.23

As shown in Table I the specific surface area was reduced considerably during the heat transfer experiments, a fact which, at first, seemed paradoxical since the particles also experienced significant attrition (see Figures 3 through 5). The effect, however, resulted from the

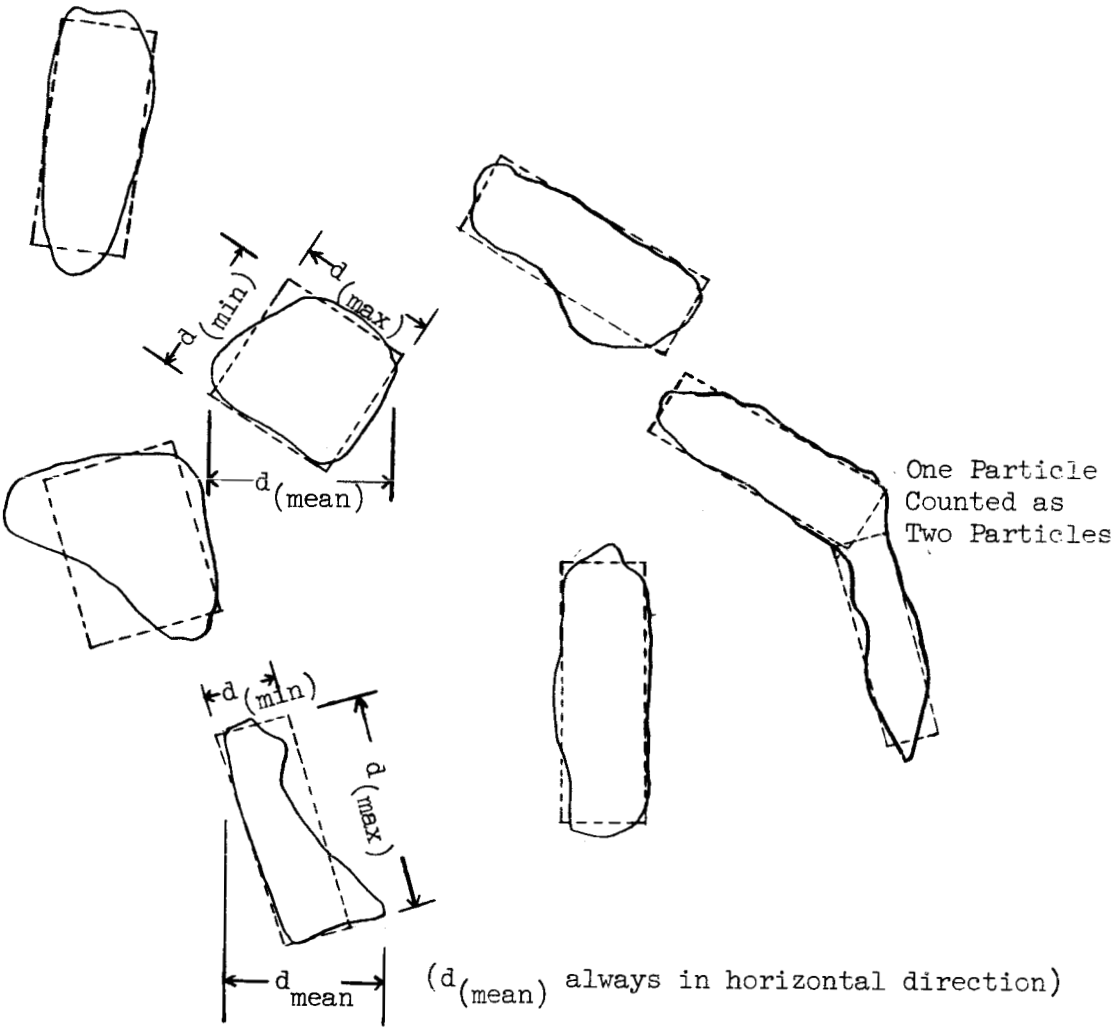

Figure 2. Measurement of Particle Geometry

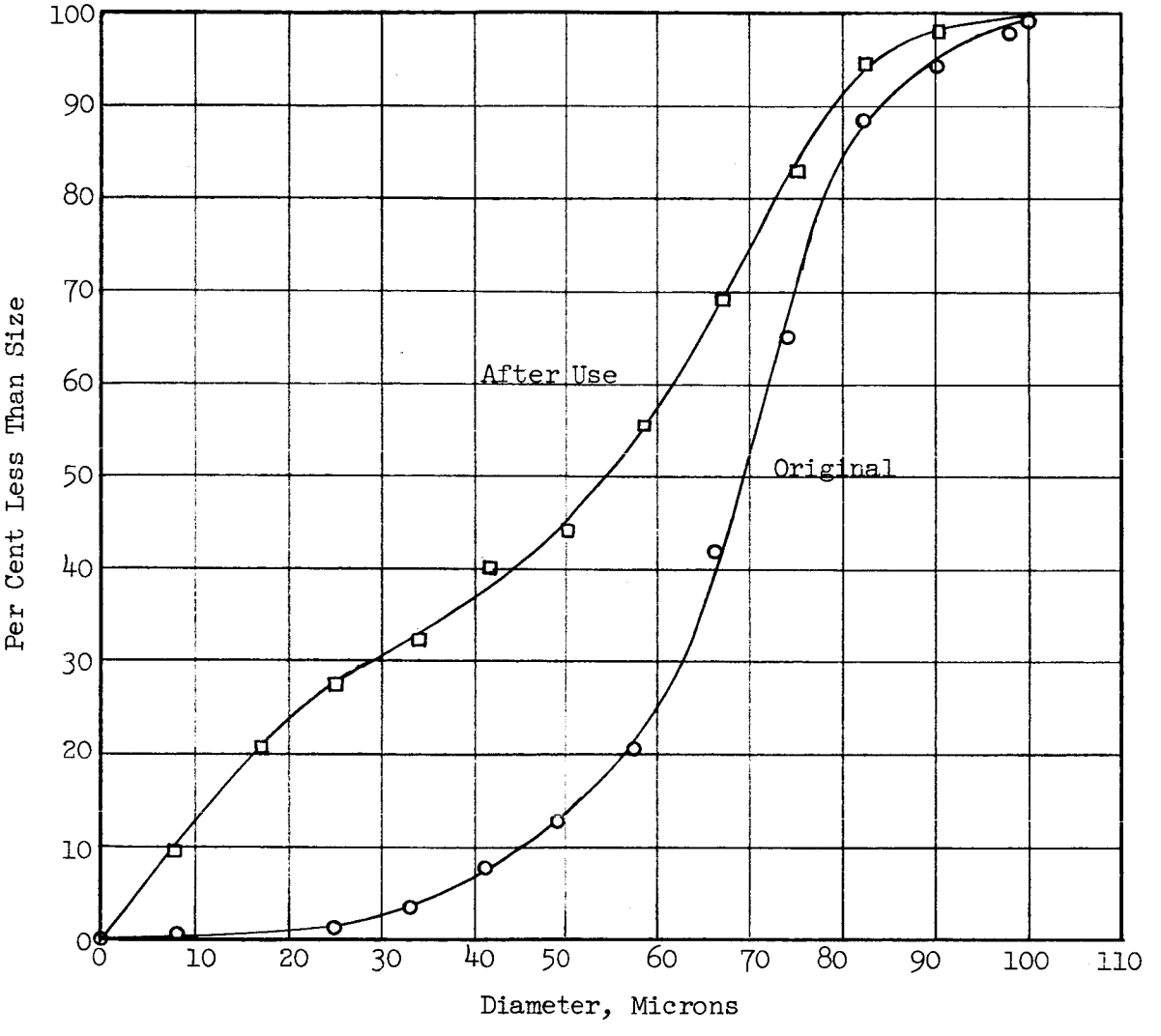

Figure 3 . Particle Size Distribution of Ferrous Sulfide, 53 -88μ Screen Size Fraction

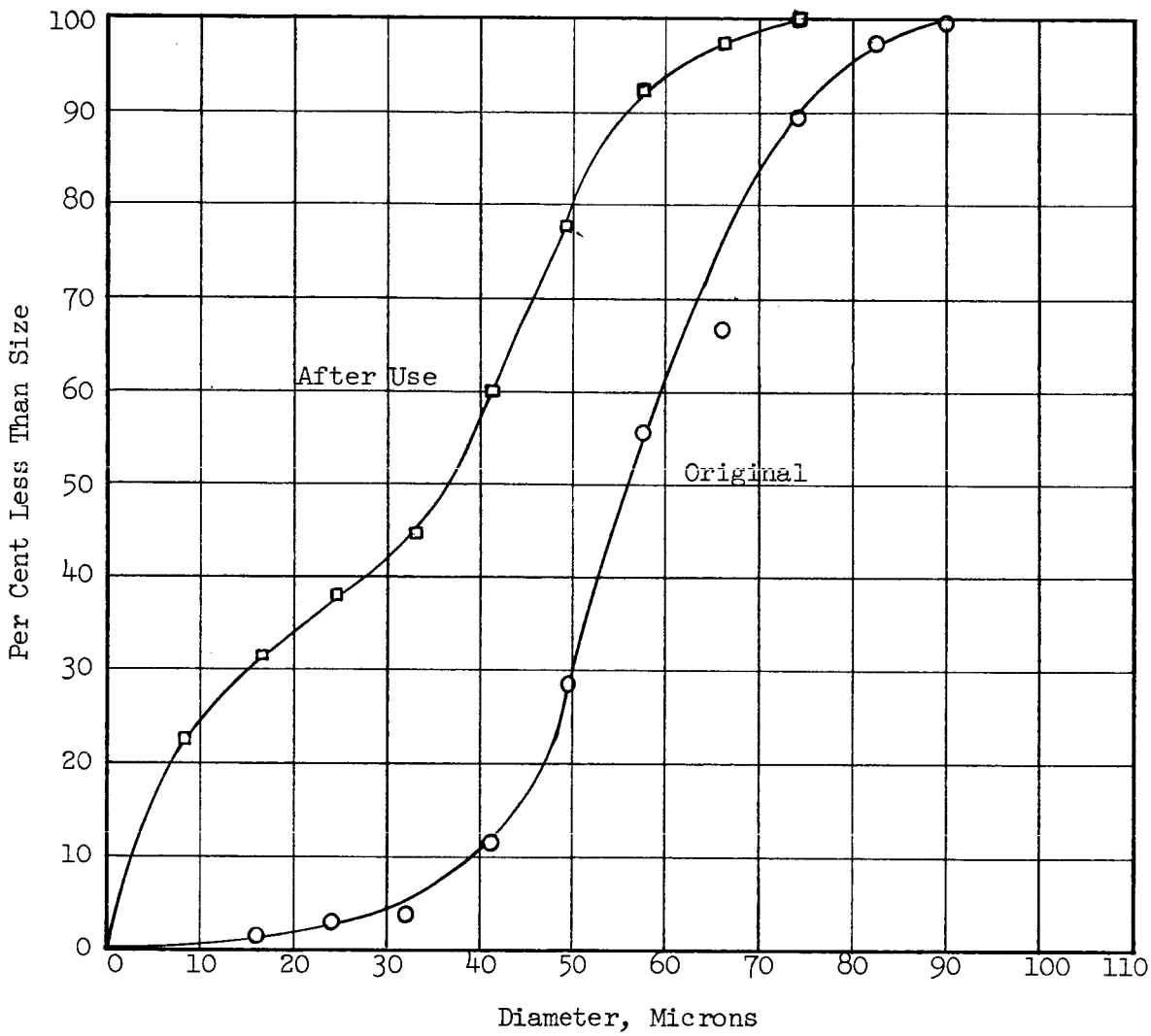

Figure 4. Particle Size Distributions of Ferrous Sulfide, 44 - 53μ Screen Size Fraction

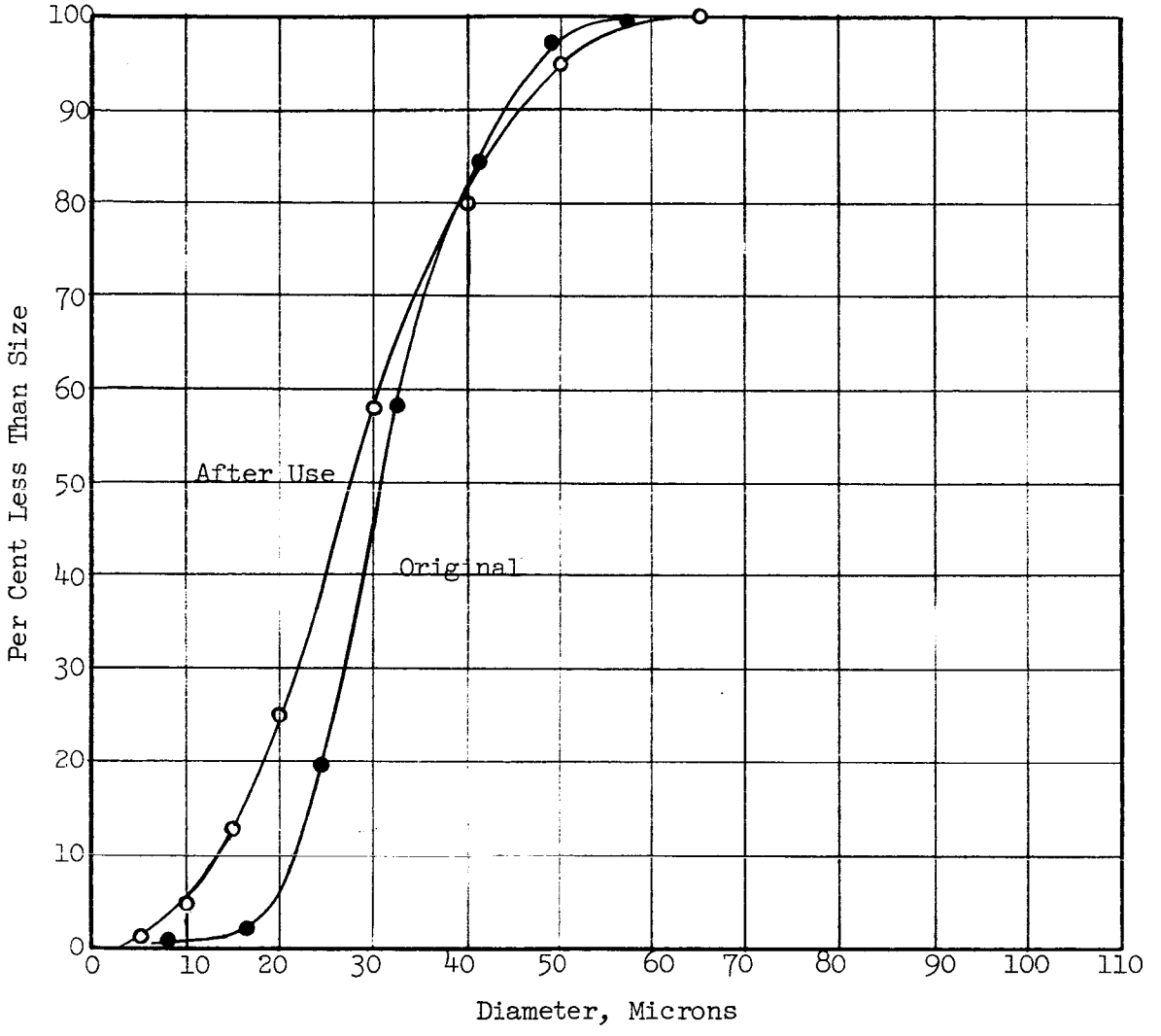

Figure 5. Particle Size Distributions of Ferrous Sulfide, 30 - 44μ Screen Size Fraction

capture in the bag filter of submicron particles which were present on the surface of the large particles in the original powder. These particles were so small they were not included in the particle size distribution. Figure 6 is a set of photographs of the original material, the continuously recirculated fraction and the portion permanently retained in the bag filter. Although particle attrition was very significant, the properties of the circulated powder fraction appeared to become acceptably constant after the first few minutes of the heat transfer experimentation and were considered valid for theoretical deductions.

The results of the length-to-diameter ratio determinations were essentially the same in all instances and are typically represented in Figure 7. It is to be noted that the distribution of ratios was independent of particle size and ranged from 1.0 to 2.2. If there had been a dependence of ℓ/d on particle size, the average particle size would have changed with ℓ/d instead of being constant as shown in Figure 7.

C. Experimental Data

1. With Water-Cooled Calorimeter

The heat transferred to a given dispersion of powder is determined from an energy balance on the system both with and without powder flow. Since the principal mode of heat transfer to the aerosol system is radiation, the difference between these two heat balances is the energy absorbed by the particles. These energy balances were derived by measuring the heat gain of the calorimeter coolant and the

(a) ORIGINAL MATERIAL

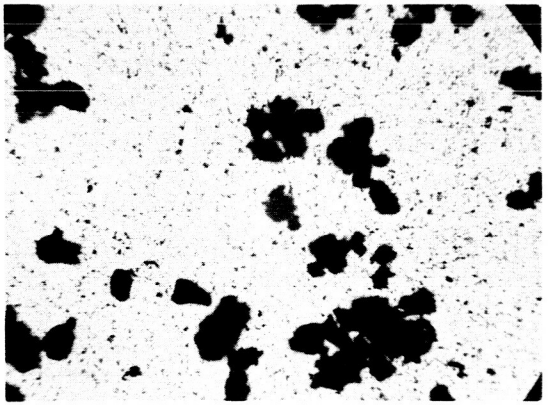

(b) MATERIAL RETAINED IN BAG FILTER

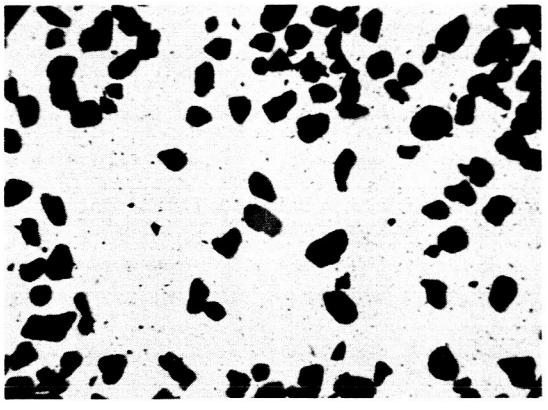

(c) CIRCULATED MATERIAL

Figure 6. Photomicrographs of FeS Powder (44 to 53 μ) Showing the Preferential Capture of the Very Small Particles in the Bag Filter. (1 cm = 186μ).

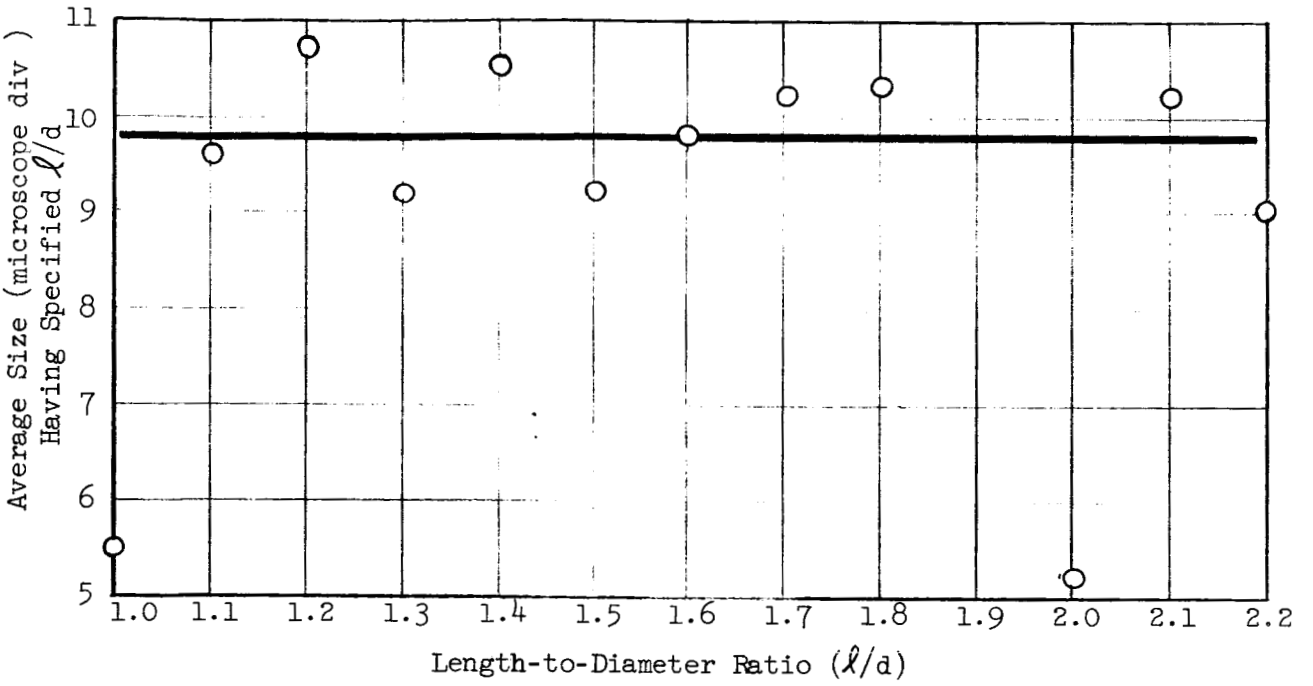

A. Data for 53 - 88μ Size Fraction

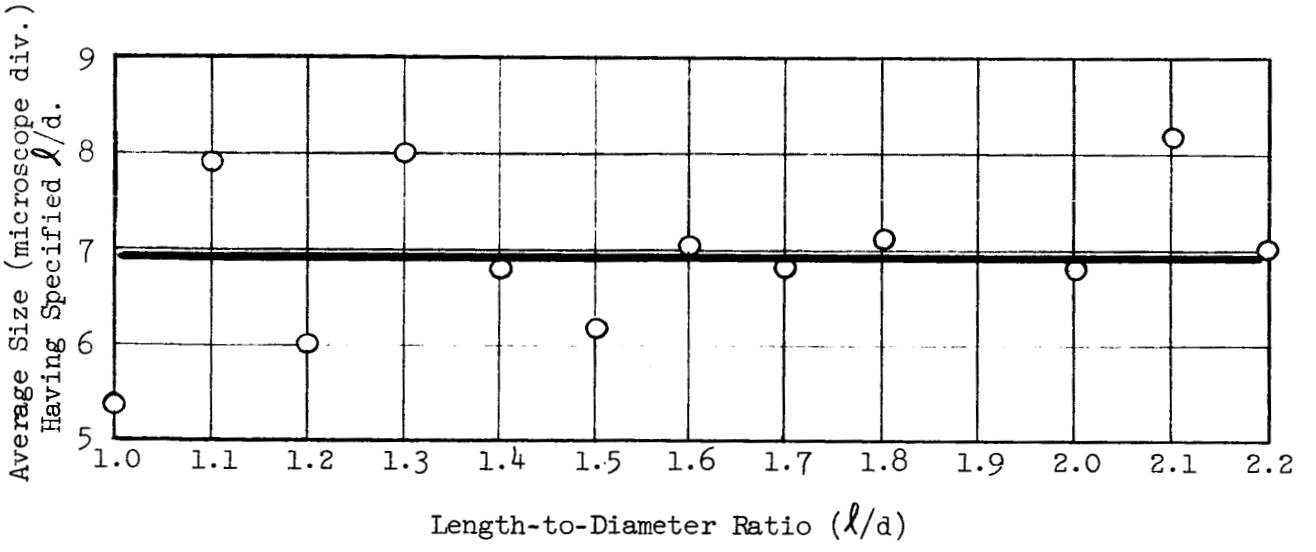

B. Data for 30 - 44μ Size Fraction

Figure 7. Average Particle Size as Function of Length-to-Diameter Ratio

heat remaining with the exit aerosol. The calorimeter and the quartz conduit in the furnace are protected from the surroundings so that heat transfer other than by radiation can be neglected. The calorimeter does not serve as the primary measure of the heat content of the aerosol. Rather it is a controlled heat sink between the furnace and the thermocouple that measures the aerosol temperature. This length of conduit is required to place the thermocouple beyond the effects of the radiant field originating in the furnace and to allow sufficient time for thermal equilibrium to be established between the particles and the gas.

For the initial experiments, water was the coolant for the calorimeter, and data were collected for the zinc powder and one of the larger size fractions of the ferrous sulfide. The experimental data for the zinc powder suspensions are presented in Table II and the calculated heat absorption is presented graphically in Figure 8. Table III and Figure 9 present similar data for the ferrous sulfide.

The tabulated data for these experiments include the temperature of the aerosol system and the calorimeter coolant; the air and powder flow rates; the furnace temperature; and, finally, the calculated enthalpy changes produced by the addition of particles to the aerosol system. The temperatures for the aerosol and the calorimeter coolant are presented directly as indicated by the thermocouples as located in Figure 1. The difference quantity, $\Delta(\Delta t)$, however, is a combination of two measurements, one being the temperature rise of the calorimeter coolant when only air was flowing in the aerosol system, and the other being the temperature with powder flow. The temperature

TABLE II

EXPERIMENTAL AND CALCULATED DATA FOR ZINC[a]

Run No.	Powder Feed Rate (lb/min)	Entering Air or Aerosol Temperature (°F)	Temperature at Calorimeter Exit		Calorimeter Coolant Temperature Rise for Air and Change in Rise When Powder Added		Enthalpy Change within Test System		
			Air (°F)	Aerosol (°F)	Air (°F)	Δ(ΔT) (°F)	Air (Btu/min)	Particles (Btu/min)	Total[b] (Btu/min)
1	0.19	78.4	106.6	126.8	7.7	+0.3	1.18	0.28	1.46
2	0.19	78.5	106.1	127.3	7.7	+0.4	1.24	0.28	1.52
3	0.19	78.8	104.3	127.1	6.7	+0.3	1.33	0.86	2.19
4	0.13	78.8	105.9	123.7	6.8	+0.3	1.04	0.55	1.59
5	0.13	83.4	112.0	129.0	7.2	0.0	0.99	0.56	1.55
6	0.19	83.6	113.7	135.0	7.3	+0.1	1.24	0.92	2.16
7	0.25	84.5	114.8	140.6	7.3	+0.5	1.50	1.30	2.80
8	0.25	85.1	115.7	139.6	7.4	+0.5	1.39	1.26	2.65
9	0.25	85.9	116.4	140.2	7.2	+0.6	1.39	1.26	2.65
10	0.13	90.9	117.9	138.3	7.4	+0.1	1.19	0.58	1.77
11	0.13	91.3	118.8	139.3	7.7	-0.1	1.20	0.59	1.79
12	0.19	91.8	118.8	144.0	7.7	+0.3	1.47	0.93	2.40
13	0.19	91.5	119.0	144.8	7.9	+0.3	1.50	0.95	2.45
14	0.13	89.8	165.7	174.0	4.6	+0.7	0.48	1.02	1.50

(Continued)

TABLE II (Continued)

EXPERIMENTAL AND CALCULATED DATA FOR ZINC[a]

Run No.	Powder Feed Rate (lb/min)	Entering Air or Aerosol Temperature (°F)	Temperature at Calorimeter Exit		Calorimeter Coolant Temperature Rise for Air and Change in Rise When Powder Added		Enthalpy Change within Test System		
			Air (°F)	Aerosol (°F)	Air (°F)	Δ(ΔT) (°F)	Air (Btu/min)	Particles (Btu/min)	Total[b] (Btu/min)
15	0.13	90.2	165.0	173.9	4.8	+0.6	0.52	1.02	1.54
16	0.13	90.6	164.8	173.9	4.8	+0.5	0.53	1.02	1.55
17	0.13	91.1	165.2	174.2	4.9	+0.3	0.52	1.01	1.53
18	0.13	89.8	111.6	133.0	3.9	+0.2	1.25	0.53	1.78
19	0.13	90.5	112.9	133.8	4.4	0.0	1.22	0.53	1.75

(a) Experiment Conditions: calorimeter coolant, water, 0.095 CFM; air flow rate for aerosol, 3.22 CFM at 1 atm, 70° F; furnace temperature 2160° F ± 10° F.

(b) Total did not include heat calculated for coolant; see text.

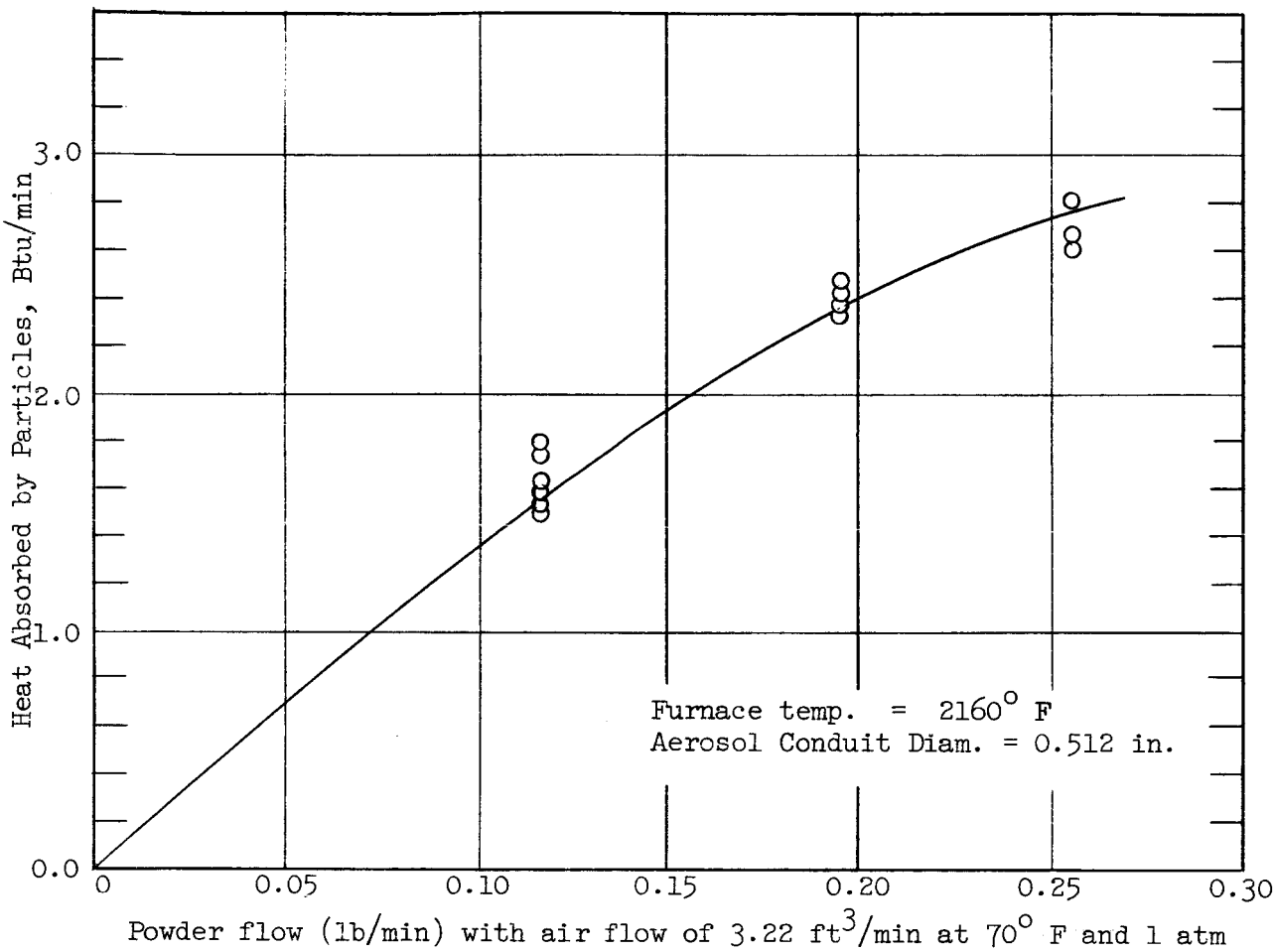

Figure 8. Radiant Energy Absorption by Zinc Particle Clouds

TABLE III

EXPERIMENTAL AND CALCULATED DATA FOR 53 - 88μ FERROUS SULFIDE[a]

Run No.	Powder Feed Rate (lb/min)	Entering Air or Aerosol Temperature (°F)	Temperature at Calorimeter Exit		Calorimeter Coolant Temperature Rise for Air and Change in Rise When Powder Added		Enthalpy Change within Test System		
			Air (°F)	Aerosol (°F)	Air (°F)	Δ(ΔT) (°F)	Air (Btu/min)	Particles (Btu/min)	Total[b] (Btu/min)
1	0.24	83.3	105.7	127.1	8.3	+1.3	1.25	1.82	3.07
2	0.24	81.9	127.1	137.7	6.7	-0.6	0.62	2.32	2.94
3	0.24	83.0	129.3	138.8	8.0	-0.5	0.55	2.32	2.87
4	0.16	82.6	130.2	140.1	7.3	+0.2	0.58	1.52	2.10
5	0.16	82.6	132.1	140.3	7.5	+0.3	0.48	1.53	2.01
6	0.089	82.2	134.2	141.1	8.1	-0.2	0.40	0.92	1.32
7	0.059	81.5	125.1	130.7	7.5	+0.1	0.33	0.49	0.82
8	0.059	81.8	126.6	132.0	7.1	+0.7	0.31	0.50	0.81
9	0.089	82.3	127.2	135.0	7.5	-0.2	0.45	0.83	1.28
10	0.16	82.5	129.3	140.2	7.4	+0.1	0.64	1.53	2.17
11	0.24	82.5	130.2	144.0	7.5	+0.1	0.80	2.55	3.35
12	0.089	82.6	132.0	140.8	8.1	-0.2	0.51	0.91	1.42
13	0.089	81.3	129.2	136.9	9.0	+0.4	0.45	0.87	1.32
14	0.089	81.8	129.3	137.8	8.6	-0.5	0.50	0.88	1.38

(Continued)

TABLE III (Continued)

EXPERIMENTAL AND CALCULATED DATA FOR 53 - 88μ FERROUS SULFIDE[a]

Run No.	Powder Feed Rate (lb/min)	Entering Air or Aerosol Temperature (°F)	Temperature at Calorimeter Exit		Calorimeter Coolant Temperature Rise for Air and Change in Rise When Powder Added		Enthalpy Change within Test System		
			Air (°F)	Aerosol (°F)	Air (°F)	Δ(ΔT) (°F)	Air (Btu/min)	Particles (Btu/min)	Total[b] (Btu/min)
15	0.16	82.6	130.2	141.7	8.9	-0.1	0.67	1.57	2.24
16	0.16	82.9	132.9	143.8	9.2	-0.2	0.64	1.61	2.25
17	0.24	83.4	133.3	147.3	8.6	+0.2	0.82	2.65	3.47
18	0.24	83.7	134.3	149.0	9.0	-0.2	0.86	2.71	3.57
19	0.059	82.9	133.2	139.3	8.9	+0.1	0.36	0.56	0.92
20	0.059	78.8	127.3	133.5	10.2	+0.2	0.36	0.55	0.91
21	0.089	79.2	128.7	137.7	11.2	+0.5	0.53	0.92	1.45
22	0.16	79.3	129.9	142.7	11.0	+0.8	0.75	1.68	2.43
23	0.24	79.9	130.2	146.0	10.2	+0.5	0.92	2.15	3.67
24	0.16	79.9	130.3	142.6	10.4	0.0	0.72	1.66	2.38
25	0.089	79.8	129.8	138.8	9.7	+0.5	0.53	0.93	1.46
26	0.059	79.6	130.3	137.1	9.9	+0.3	0.40	0.58	0.98

(a) Experiment Conditions: calorimeter coolant, water, 0.095 CFM; air flow rate for aerosol, 3.22 CFM at 1 atm, 70° F; furnace temperature 2160° F ± 10° F.

(b) Total did not include heat calculated for coolant; see text.

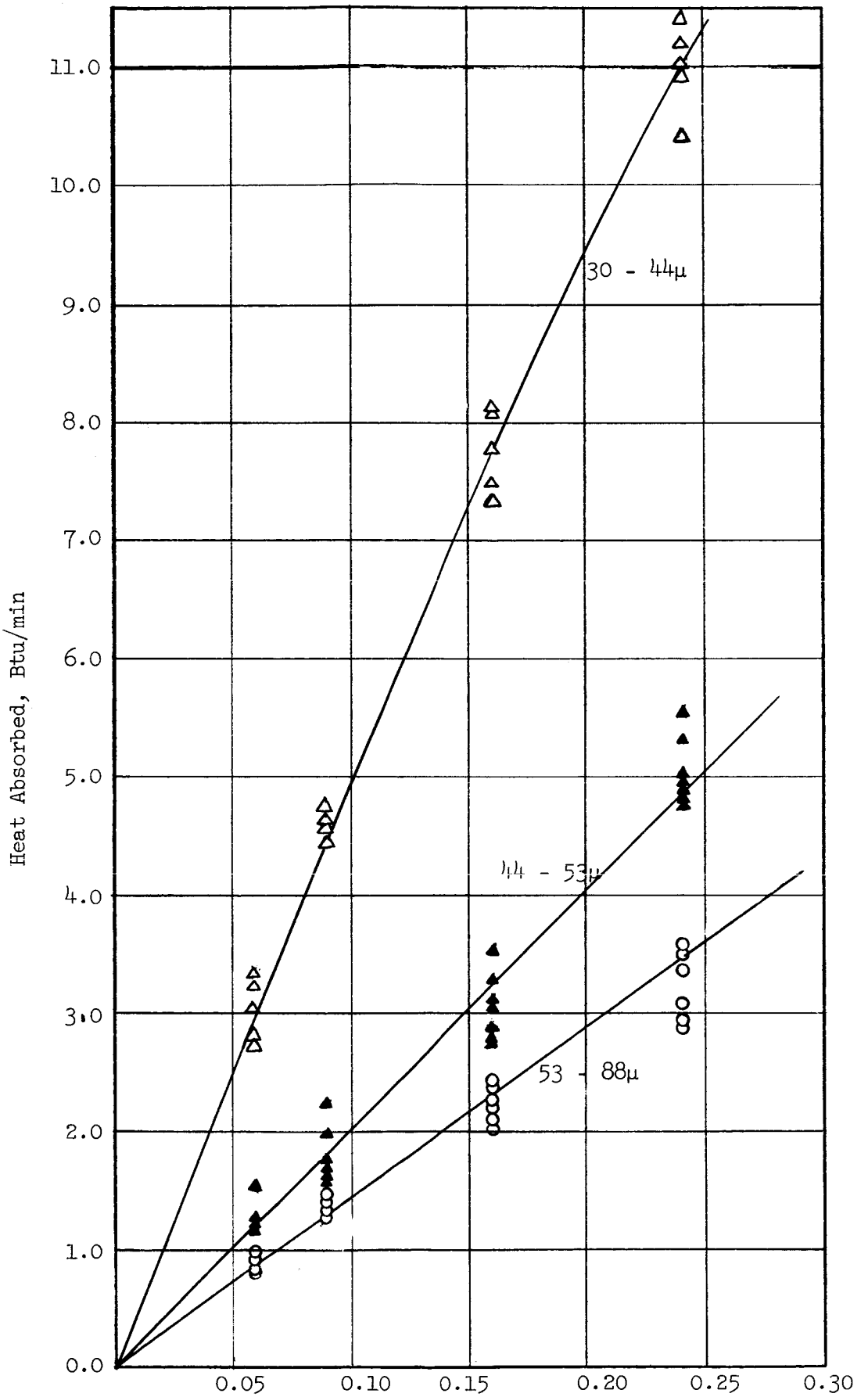

Figure 9. Radiant Energy Absorption by Ferrous Sulfide Particle Clouds

rise of the calorimeter coolant was a temperature difference, hence the notation, Δt. The difference between these two Δt quantities, however, represents the temperature change of the calorimeter coolant when particles were added to the system. The second difference was represented by $\Delta(\Delta t)$. It should be noted that this quantity was in some cases positive and in others negative, depending on whether more or less heat was absorbed by the calorimeter when particles were added to the system.

The enthalpy data are for the changes of the respective systems when particles were added to the air stream to form aerosols. For these experiments with water as the calorimeter coolant the contribution of the enthalpy change was relatively large and it also resulted from a small temperature difference between two large temperature rises. This condition together with the high heat capacity of water gave an appreciable uncertainty to the evaluation of this quantity.

Since data for these initial experiments exhibited wide variation as well as a sizeable uncertainty in the heat removed by the calorimeter, it was decided to install an additional thermocouple in the aerosol stream and with this additional temperature measurement to make heat balances exclusively on the aerosol systems. These measurements, however, did not yield meaningful results because of radiation effects on the new thermocouple. Even though the sensing element was 7 inches within the calorimeter, it was significantly influenced by radiation from the furnace. With no particle flow, the thermocouple received some radiation and with increasing particle concentration received

monatonically greater shielding and less radiation. From energy balance calculations on the calorimeter it appeared that at low particle concentrations too high a temperature was indicated by the thermocouple while at the higher ones the temperature was too low.

Although the temperature measurements near the entrance of the calorimeter did not give exact results, they were helpful in studying the heat transfer characteristics of the calorimeter. From these data log-mean temperature differences between the coolant and the aerosol system were calculated. These differences were very nearly the same both with and without powder flow. Further, if it is accepted that the presence of particles increases the overall heat transfer coefficient by about 8 per cent (1), the heat transferred ($UA\Delta T$) to the coolant in each case was essentially the same. The $\Delta(\Delta t)$, then, should have been zero. Thus, it was assumed that the calorimeter absorbed the same amount of heat with and without powder and the enthalpy change shown for the coolant was disregarded. These are the results shown on Figures 8 and 9 for the zinc and 53 to 88 micron ferrous sulfide aerosols. Subsequent data with other ferrous sulfide powders, also shown in Figure 9, support this conclusion.

2. With Air-Cooled Calorimeter

For optimum operation the calorimeter should be at approximately room temperature and thus reduce to a minimum extraneous heat effects from the surroundings. For this purpose water would be a

(1) L. Farbar and M. J. Morley, "Heat Transfer to Flowing Gas-Solids Mixtures in a Circular Tube," Ind. Eng. Chem. 49, No. 7, 1143-50 (1957).

better coolant due to its sizeable heat capacity. Its use is actually a disadvantage, however, in evaluating, with acceptable precision, the amount of energy absorbed by the water. When the water rate is sufficiently high to provide stable operation the temperature differences involved are too small to evaluate satisfactorily; and when the water rate is reduced to give measurable temperatures, the calorimeter is not thermally stable and too much time is required for equilibration.

To achieve better measurements and more stable operation, air was used as the calorimeter coolant for the remaining experiments with ferrous sulfide. The data collected under these conditions appear to be the most reliable thus far. The results are presented in Tables IV and V and the calculated energies absorbed by the particle-cloud are shown graphically in Figure 9. The absorption measurements were reproducible within ± 0.5 Btu/min and there was a considerable reduction in the uncertainty of the heat removed by the calorimeter in comparison with the experiments performed with water as the cooling medium.

3. Without Cooling

Other experiments were conducted in which the calorimeter was replaced with a length of well-insulated tubing and measurements of the aerosol's temperature upon issuing from the furnace were attempted. The tubing, as with the calorimeter, was sufficiently long for radiation from the furnace not to affect the thermocouple measuring the aerosol's temperature. This procedure was unsuccessful since radiation entering the insulated portion of the aerosol conduit caused the temperature there to increase slowly with time and the period required for equilibrium to be established was too long for practical operation.

TABLE IV

EXPERIMENTAL AND CALCULATED DATA FOR 44 - 53μ FERROUS SULFIDE[a]

Run No.	Powder Feed Rate (lb/min)	Entering Air or Aerosol Temperature (°F)	Temperature at Calorimeter Exit		Calorimeter Coolant Temperature Rise for Air and Change in Rise When Powder Added		Enthalpy Change withing Test System			
			Air (°F)	Aerosol (°F)	Air (°F)	Δ(ΔT) (°F)	Air (Btu/min)	Particles (But/min)	Coolant (Btu/min)	Total (Btu/min)
1	0.089	81.7	158.8	167.3	41.6	+0.9	0.55	1.30	0.12	1.97
2	0.16	82.6	159.5	171.2	42.5	+0.1	0.75	2.35	0.01	3.11
3	0.24	82.9	160.6	180.1	43.4	+0.5	1.26	4.00	0.07	5.33
4	0.16	83.2	159.7	174.2	43.3	+1.3	0.93	2.41	0.17	3.51
5	0.089	83.3	159.2	170.3	43.0	+1.5	0.71	1.32	0.20	2.23
6	0.059	83.4	158.4	166.6	42.5	+1.2	0.53	0.83	0.16	1.52
7	0.059	79.4	151.1	158.3	30.4	+0.3	0.40	0.79	+0.04	1.23
8	0.24	79.8	156.0	174.4	41.0	-0.3	1.19	3.90	-0.04	5.04
9	0.24	79.9	154.0	176.9	40.3	+0.5	1.48	4.00	+0.07	5.55
10	0.24	80.0	155.7	174.2	41.6	-0.7	1.19	3.88	-0.10	4.97
11	0.24	81.0	156.4	174.2	41.8	-0.8	1.15	3.84	-0.12	4.87
12	0.24	81.0	156.4	174.2	41.9	-1.1	1.15	3.84	-0.16	4.82
13	0.24	81.2	156.8	174.4	42.6	-1.1	1.13	3.84	-0.16	4.81
14	0.24	81.2	157.6	176.0	42.5	-1.2	1.19	3.91	-0.18	4.91

(Continued)

TABLE IV (Continued)

EXPERIMENTAL AND CALCULATED DATA FOR 44 - 53μ FERROUS SULFIDE[a]

Run No.	Powder Feed Rate (lb/min)	Entering Air or Aerosol Temperature (°F)	Temperature at Calorimeter Exit		Calorimeter Coolant Temperature Rise for Air and Change in Rise When Powder Added		Enthalpy Change within Test System			
			Air (°F)	Aerosol (°F)	Air (°F)	Δ(ΔT) (°F)	Air (Btu/min)	Particles (Btu/min)	Coolant (Btu/min)	Total (Btu/min)
15	0.24	81.6	158.6	177.3	42.8	-1.2	1.20	3.94	-0.18	4.97
16	0.16	81.4	160.0	173.3	43.9	-0.1	0.86	2.44	-0.02	3.28
17	0.16	81.5	157.6	169.8	42.7	+0.2	0.79	2.34	-0.03	3.10
18	0.16	81.6	157.6	167.2	42.2	-0.6	0.62	2.27	-0.09	2.80
19	0.16	81.7	158.3	168.9	42.5	-0.8	0.69	2.31	-0.12	2.88
20	0.16	81.7	158.8	169.3	42.5	-0.8	0.68	2.32	-0.12	2.88
21	0.16	81.8	158.3	167.7	42.1	-0.8	0.61	2.28	-0.12	2.76
22	0.16	81.9	159.2	168.4	42.5	-1.0	0.59	2.29	-0.15	2.74
23	0.16	82.0	160.5	170.4	43.2	-1.2	0.64	2.34	-0.18	2.80
24	0.16	82.1	160.7	170.4	43.3	-1.1	0.63	2.34	-0.16	2.80
25	0.16	82.2	160.0	160.3	43.1	-0.9	0.60	2.31	-0.13	2.78
26	0.089	82.5	160.9	168.9	43.7	-0.5	0.52	1.31	-0.07	1.75
27	0.089	82.7	162.2	169.8	44.2	-0.5	0.49	1.32	-0.07	1.74
28	0.089	82.5	160.9	168.1	43.6	-0.3	0.46	1.30	-0.04	1.72
29	0.089	82.7	161.3	168.9	43.6	-0.4	0.49	1.31	-0.06	1.74

(Continued)

TABLE IV (Concluded)

EXPERIMENTAL AND CALCULATED DATA FOR 44 - 53μ FERROUS SULFIDE[a]

Run No.	Powder Feed Rate (lb/min)	Entering Air or Aerosol Temperature (°F)	Temperature at Calorimeter Exit		Calorimeter Coolant Temperature Rise for Air and Change in Rise When Powder Added		Enthalpy Change within Test System			
			Air (°F)	Aerosol (°F)	Air (°F)	Δ(ΔT) (°F)	Air (Btu/min)	Particles (Btu/min)	Coolant (Btu/min)	Total (Btu/min)
30	0.089	82.7	161.3	168.9	43.2	+0.6	0.49	1.31	-0.06	1.74
31	0.089	82.7	161.7	168.4	43.4	-0.5	0.43	1.30	-0.07	1.66
32	0.089	82.9	161.7	168.9	43.4	-0.2	0.46	1.31	-0.03	1.74
33	0.089	83.0	162.2	167.7	43.0	-0.5	0.35	1.29	-0.07	1.57
34	0.089	83.4	163.3	170.4	43.9	-0.9	0.46	1.32	-0.13	1.65
35	0.059	83.4	162.6	168.4	44.4	-0.1	0.37	0.85	-0.02	1.21
36	0.059	83.4	162.6	168.1	44.1	+0.2	0.35	0.85	+0.03	1.23
37	0.059	83.4	163.3	169.0	43.9	+0.1	0.37	0.86	+0.02	1.24
38	0.059	83.4	163.7	169.3	43.7	+0.2	0.36	0.85	+0.03	1.24
39	0.059	83.1	163.2	168.7	43.2	+0.2	0.35	0.86	+0.03	1.24
40	0.059	82.9	163.2	168.7	43.2	+0.1	0.35	0.86	+0.02	1.23
41	0.059	82.9	162.6	168.0	42.8	0.0	0.35	0.85	0.00	1.17
42	0.059	82.9	162.2	167.7	43.0	-0.2	0.35	0.85	-0.03	1.17

(a) Experiment Conditions: calorimeter coolant, air, 6.70 CFM at 1 atm, 70° F; air flow rate for aerosol, 3.22 CFM at 1 atm, 70° F; furnace temp 2160° F ± 10° F.

TABLE V

EXPERIMENTAL AND CALCULATED DATA FOR 30 - 44μ FERROUS SULFIDE[a]

Run No.	Powder Feed Rate (lb/min)	Entering Air or Aerosol Temperature (°F)	Temperature at Calorimeter Exit		Calorimeter Coolant Temperature Rise for Air and Change in Rise When Powder Added		Enthalpy Change within Test System			
			Air (°F)	Aerosol (°F)	Air (°F)	Δ(ΔT) (°F)	Air (Btu/min)	Particles (Btu/min)	Coolant (Btu/min)	Total (Btu/min)
1	0.059	79.3	165.8	183.5	44.7	+3.3	1.26	1.06	0.49	2.80
2	0.059	79.3	167.7	187.2	46.8	+2.7	1.26	1.08	0.40	2.73
3	0.059	79.3	168.6	189.8	47.3	+3.8	1.37	1.11	0.56	3.03
4	0.24	79.4	168.6	229.3	47.1	+7.8	3.91	6.18	1.15	11.2
5	0.24	79.5	169.3	228.7	47.5	+6.2	3.83	6.15	0.91	10.9
6	0.24	80.3	171.3	230.6	48.2	+6.8	3.82	6.19	1.00	11.0
7	0.24	80.3	172.7	234.0	48.8	+7.7	3.95	6.34	1.10	11.4
8	0.16	80.3	175.2	225.6	50.3	+7.0	3.25	3.85	1.00	8.13
9	0.16	80.0	178.9	227.6	52.5	+5.0	3.14	3.91	0.74	7.78
10	0.16	80.0	181.7	228.7	50.0	+8.2	3.03	3.94	1.2	8.18
11	0.16	80.0	179.9	224.5	52.0	+5.0	2.87	3.83	0.77	7.48
12	0.089	80.0	180.4	211.7	52.5	+4.9	2.02	2.00	0.72	4.74
13	0.089	80.0	181.0	211.0	52.2	+4.8	1.93	1.99	0.71	4.63
14	0.089	80.0	182.0	210.0	53.0	+4.4	1.80	1.98	0.65	4.42

(Continued)

TABLE V (Continued)

EXPERIMENTAL AND CALCULATED DATA FOR 30 - 44μ FERROUS SULFIDE[a]

Run No.	Powder Feed Rate (lb/min)	Entering Air or Aerosol Temperature (°F)	Temperature at Calorimeter Exit		Calorimeter Coolant Temperature Rise for Air and Change in Rise When Powder Added		Enthalpy Change within Test System			
			Air (°F)	Aerosol (°F)	Air (°F)	Δ(ΔT) (°F)	Air (Btu/min)	Particles (Btu/min)	Coolant (Btu/min)	Total (Btu/min)
15	0.089	80.0	186.3	216.7	54.4	+4.7	1.96	2.08	0.69	4.73
16	0.059	80.0	186.1	207.9	54.9	+3.8	1.40	1.28	0.56	3.24
17	0.059	80.0	188.1	209.7	54.8	+4.4	1.39	1.30	0.65	3.34
18	0.089	79.6	190.6	219.4	56.5	+4.1	1.86	2.13	0.60	4.58
19	0.16	81.4	193.7	235.3	59.0	+3.9	2.86	4.08	0.57	7.33
20	0.24	81.0	196.6	245.1	60.4	+3.8	3.12	6.76	0.56	10.4

(a) Experiment Conditions: calorimeter coolant, air, 7.51 CFM at 1 atm, 70° F; air flow rate for aerosol, 3.22 CFM at 1 atm, 70° F; furnace temp 2160° F ± 10° F.

D. Determination of Radiant Flux in Radiation Field

1. Device for Measuring Flux

A measure of the radiation flux within the aerosol system is required if the efficiency of a particle as a radiation absorber is to be evaluated. This quantity, therefore, is also being measured. The procedure employed is to expose a thermocouple bead to the radiation within the quartz tube and to calculate the energy absorbed by it from a knowledge of its temperature, the convective heat transfer coefficient to the surrounding air, and the temperature of the free stream. From this quantity, the view factors between the bead and the furnace walls, and the emissive properties of the two, the intensity of the radiant field can be calculated. Figure 10 is a pictorial description of the device utilized.

A bead of 0.130 inch diameter was supported in the center of the air stream well away from objects significantly shading it from radiation. The bead diameter was large compared to the size of the supporting thermocouple leads so their effect on its energy balance could be neglected. The bead's diameter was accurately determined so that the convective heat transfer coefficient to the surrounding air stream could be evaluated.

A shielded thermocouple with an air intake 1.5 inches above the exposed thermocouple measured the free-stream air temperature. Two shields were employed, the outer of which was cooled with air being forced through it by the main stream. The inner shield was cooled by air drawn through it with a laboratory aspirator. An end shield, as shown in the figure, partially covered the end of the outer shield

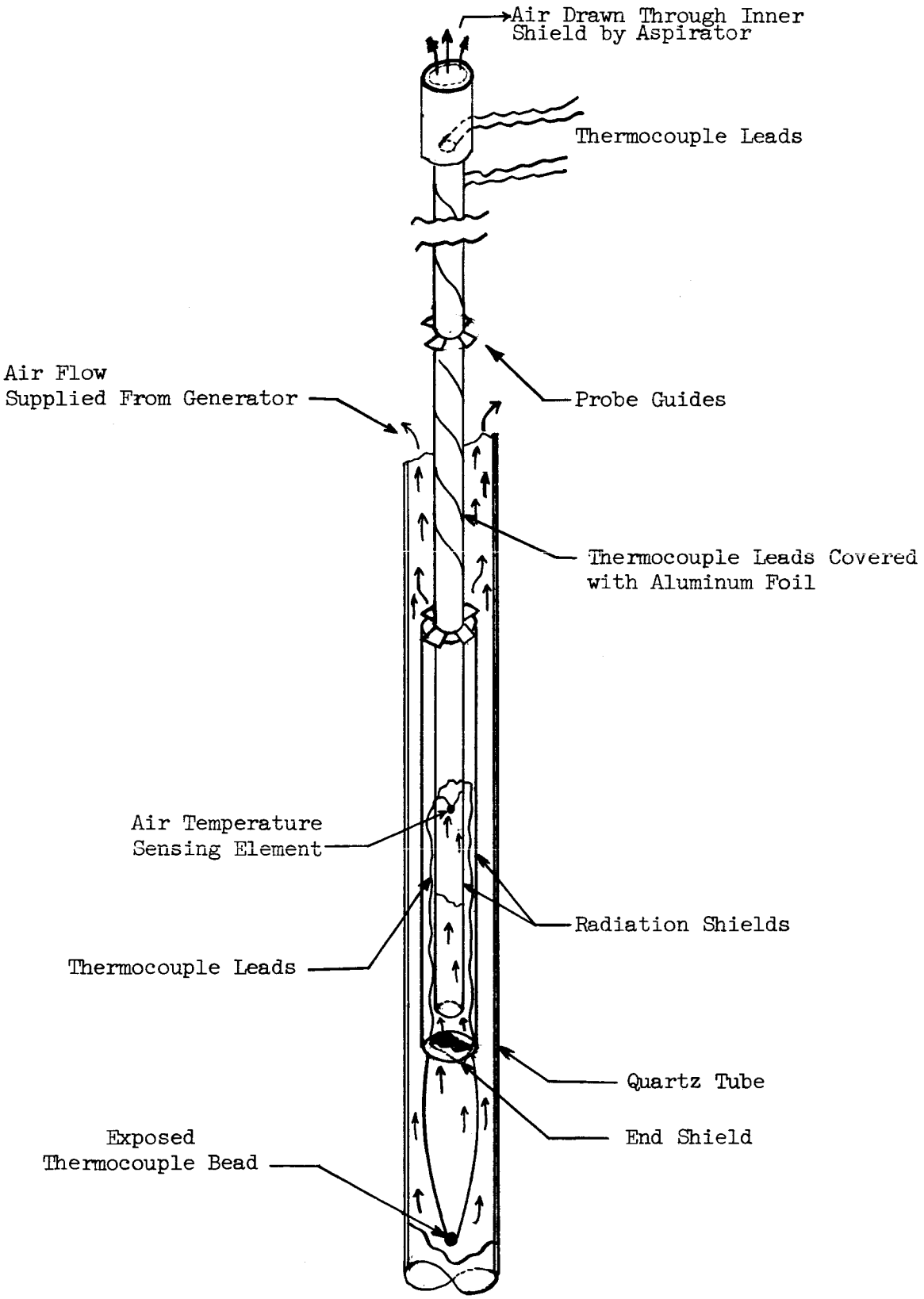

Figure 10. Probe for Measuring Air Temperature and Radiation Flux in Furnace

so that direct radiation could not enter the inner one. The protected thermocouple was located at the center and about the midpoint between the ends of the shields. The temperature indicated by the shielded thermocouple is taken to be that of the free stream air at the end of the shield.

The tubing forming the inner shield was extended upward to provide means for positioning the probe. Guides along its length kept the unit centered in the quartz conduit. Leads to the protected thermocouple were passed through the extended tubing while those to the exposed thermocouple were wrapped around the outside and covered with aluminum foil to protect them from radiation.

2. Measurements

Measurements along the axis of the quartz tube were made to obtain the exposed-thermocouple temperature and the free-stream air temperature. The furnace was brought to an operating temperature of 2160° F $\pm$ 10° to make these determinations, and a measured air flow rate was established in the conduit. Then, the temperatures along the axis of the furnace were measured at one inch intervals. At each position a series of about 20 readings was made to give a good average value; variations on the order of $\bullet$ 6° F were recorded. The data are presented in Tables VI and VII. The depth of the exposed thermocouple was an integral number of inches from the top of the quartz tube while the shielded thermocouple was offset 1.5 inches due to the arrangement of the two thermocouples in the probe. To make the readings for the two thermocouples correspond to a given position within the furnace, the temperature profile of the shielded thermocouple had to be displaced 1.5 inches downward.

TABLE VI

EXPERIMENTAL DATA FOR DETERMINING RADIATION FLUX WITH AIR FLOW OF 3.22 CFM AT 1 ATM AND 70° F

Position[a]	Run 1 (mv)	Run 2 (mv)	Run 3 (mv)	Run 4 (mv)	Average of Runs (mv)	Average Thermocouple Temperature (°F)
	Exposed Thermocouple[b] Temperature as EMF with 32° F Reference Junction					
2	6.16	5.66	5.68	5.77	5.82	270.0
3	8.65	7.50	7.27	8.46	7.97	346.9
4	10.24	8.16	8.20	8.97	8.89	378.6
5	9.69	8.70	8.50	8.44	8.83	376.6
6	8.87	8.70	8.52	8.37	8.62	369.3
7	8.16	8.40	8.30	8.21	8.27	357.2
8	7.89	8.30	8.10	8.00	8.07	350.3
9	7.92	8.45	7.83	7.79	8.00	347.9
10	7.91	8.03	7.88	7.55	7.84	342.4
11	7.24	7.31	7.12	7.45	7.28	322.5
12	6.45	6.45	6.26	6.75	6.47	293.7
13	5.74	5.72	5.35	5.53	5.60	261.9
14	4.81	4.77	4.50	4.57	4.69	224.5
15	--	3.13	3.05	3.16	3.11	166.3
16	--	1.41	1.37	1.35	1.38	94.0
17	--	0.65	0.68	0.62	0.65	61.9
18	--	0.46	0.44	0.42	0.44	52.3
19	--	--	0.35	0.35	0.35	48.2
	Shielded Thermocouple[b] Temperature as EMF with 32° F Reference Junction					
0.5	4.22	4.10	4.01	4.01	4.09	205.0
1.5	4.36	4.08	4.02	4.37	4.21	209.8
2.5	4.29	4.02	3.87	4.55	4.18	208.7
3.5	3.99	3.75	3.73	3.90	3.84	195.3

(Continued)

TABLE VI (Continued)

EXPERIMENTAL DATA FOR DETERMINING RADIATION FLUX WITH AIR FLOW OF 3.22 CFM AT 1 ATM AND 70° F

Position[a]	Run 1 (mv)	Run 2 (mv)	Run 3 (mv)	Run 4 (mv)	Average of Runs (mv)	Average Thermocouple Temperature (°F)
	Shielded Thermocouple[b] Temperature as EMF with 32° F Reference Junction					
4.5	4.00	3.70	3.48	4.00	3.79	193.3
5.5	3.85	3.57	3.34	3.64	3.60	185.8
6.5	3.25	3.46	3.25	3.33	3.32	174.7
7.5	3.09	3.20	2.96	2.97	3.06	164.0
8.5	3.08	2.99	2.89	2.83	2.95	159.7
9.5	2.75	2.87	2.67	2.63	2.73	150.7
10.5	2.25	2.40	2.21	2.36	2.31	133.3
11.5	1.87	1.90	1.95	2.08	1.95	118.3
12.5	1.61	1.56	1.55	1.72	1.61	104.1
13.5	--	1.23	1.21	1.30	1.25	88.0
14.5	--	0.96	0.95	0.95	0.95	75.3
15.5	--	0.65	0.62	0.59	0.62	60.0
16.5	--	0.43	0.41	0.38	0.41	50.9
17.5	--	--	0.35	0.35	0.35	48.2

(a) Inches from top of quartz conduit; furnace extremities were at 3 inches and 15.5 inches.
(b) Copper-constantan thermocouple

TABLE VII

EXPERIMENTAL DATA FOR DETERMINING RADIATION FLUX WITH AIR FLOW 4.48 CFM AT 1 ATM AND 70° F

Position[a]	Run 1 (mv)	Run 2 (mv)	Run 3 (mv)	Average of Runs (mv)	Average Thermocouple Temperature (°F)
	Exposed Thermocouple[a] Temperature as EMF with 32° F Reference Junction				
2	4.40	4.52	4.55	4.49	220.7
3	6.41	6.44	6.42	6.42	291.9
4	6.91	6.97	7.22	7.03	313.8
5	6.69	7.02	7.07	6.93	310.3
6	6.59	6.48	6.71	6.59	298.1
7	6.42	6.40	6.47	6.43	292.2
8	6.29	6.30	6.26	6.28	286.8
9	6.25	6.15	6.04	6.15	282.1
10	6.06	6.12	6.07	6.08	279.6
11	5.55	6.08	5.87	5.83	270.4
12	5.09	5.47	5.20	5.25	248.9
13	4.40	4.60	4.44	4.48	220.0
14	4.38	3.87	3.75	4.00	201.6
15	3.68	2.82	2.57	3.02	162.3
16	2.54	1.12	1.14	1.60	103.4
17	1.15	0.55	0.50	0.73	75.5
18	0.54	0.39	0.37	0.56	57.7
19	0.42	--	--	0.42	51.4
	Shielded Thermocouple[b] Temperature as EMF with 32° F Reference Junction				
0.5	3.16	3.04	3.05	3.08	164.9
1.5	3.32	3.35	3.30	3.32	174.7
2.5	3.34	3.55	3.64	3.50	181.8

(Continued)

TABLE VII (Continued)

EXPERIMENTAL DATA FOR DETERMINING RADIATION FLUX WITH AIR FLOW OF 4.48 CFM AT 1 ATM AND 70° F

Position[a]	Run 1 (mv)	Run 2 (mv)	Run 3 (mv)	Average of Runs (mv)	Average Thermocouple Temperature (°F)
	Shielded Thermocouple[b] Temperature as EMF with 32° F Reference Junction				
3.5	2.95	3.47	3.10	3.17	168.6
4.5	2.84	3.13	2.95	2.97	160.4
5.5	2.71	2.67	2.72	2.70	149.3
6.5	2.51	2.39	2.33	2.41	137.4
7.5	2.33	2.19	2.15	2.22	129.6
8.5	2.29	2.14	2.09	2.17	127.6
9.5	2.15	1.95	1.90	2.00	120.2
10.5	1.71	1.80	1.85	1.79	111.5
11.5	1.46	1.77	1.65	1.63	104.7
12.5	1.49	1.38	1.24	1.37	93.6
13.5	1.23	1.02	0.94	1.06	80.6
14.5	0.97	0.76	0.73	0.82	69.5
15.5	0.77	0.52	0.48	0.59	59.1
16.5	0.54	0.35	0.34	0.41	50.9
17.5	0.40	--	--	0.40	50.5

(a) Inches from top of quartz conduit, furnace extremities were at 3 inches and 15.5 inches.
(b) Copper constantan thermocouple

Since the results of the experiment were directly influenced by the exact evaluation of the convective heat transfer coefficient from the exposed thermocouple and this, in turn, was significantly a function of the flow rate, data for two different flow rates were collected. The accuracy in evaluating the required heat transfer coefficient can, therefore, be judged. Further, multiple sets of data were taken to study the reproducibility of the experimental procedures.

3. Calculated Results

The exposed thermocouple assumed a temperature so that the absorption of radiation by the bead was equal to the heat loss by convection. Thus,

$$Q_r = Q_c = h \cdot A \cdot \Delta t$$

The heat flux, then, was

$$q_r = q_c = h \cdot \Delta t$$

Further, since this heat flux was the absorbed portion of the radiation impinging on the thermocouple bead, the radiation intensity of the field can be determined.

Before beginning the calculations, the temperature of the exposed and the shielded thermocouple were arranged according to position within the furnace as shown in Tables VIII and IX. Then, at each position, the flow rate of the air was adjusted to compensate for the changing temperatures along the axis of the quartz tube. Other properties of

TABLE VIII

CALCULATED HEAT ABSORBED BY RADIATION WITH AIR FLOW OF 3.22 CFM AT 1 ATM AND 70° F

Axial Distance From Top of Furnace (in)	Free Air Stream Temperature (°F)	Exposed Thermocouple Temperature (°F)	Heat Transfer Coefficient for Exposed Thermocouple (Btu/hr ft²°F)	Net Heat Flux (Btu/hr ft²)
0	205	345	44.3	6210
1	197	379	44.1	8030
2	189	377	43.9	8250
3	179	368	43.5	8250
4	169	358	43.0	8130
5	162	350	42.8	8050
6	154	347	42.6	8230
7	141	342	42.1	8460
8	127	323	41.5	8140
9	111	299	41.1	7730
10	96	264	40.5	6800
11	81	232	39.8	5650
12	67	166	39.4	3900
12.5	60	128	39.1	2660

TABLE IX

CALCULATED HEAT ABSORBED BY RADIATION WITH AIR FLOW OF 4.48 CFM AT 1 ATM AND 70° F

Axial Distance From Top of Furnace (in)	Free Air Stream Temperature (°F)	Exposed Thermocouple Temperature (°F)	Heat Transfer Coefficient for Exposed Thermocouple (Btu/hr ft²°F)	Net Heat Flux (Btu/hr ft²)
0	178	292	50.5	5760
1	165	314	50.2	7480
2	153	309	49.5	7720
3	141	298	50.0	7690
4	132	290	48.6	7670
5	128	285	48.4	7600
6	125	282	48.2	7570
7	119	279	48.0	7680
8	109	272	47.6	7750
9	98	258	47.1	7530
10	86	232	46.7	6820
11	74	200	46.2	5820
12	64	163	45.7	4530
12.5	59	132	45.5	3320

the system including the varying physical properties of the air and the characteristic Reynolds and Nusselt numbers were calculated. With these data and the heat transfer correlations presented by Bird, Stewart, and Lightfoot (2) for spheres suspended in a flowing gas, the average heat transfer coefficient, h, was evaluated. Finally, this quantity multiplied by the temperature difference, Δt, yielded the heat flux absorbed by the thermocouple bead.

The results are not final since the absorptivity of the thermocouple, needed in the calculation of the impinging radiation intensity, has not yet been determined. Experiments, however, are presently being planned to accomplish this. Although the absorptivity of the bead is not presently known, the data do show the variation of radiation intensity within the field. It is low at the bottom of the furnace as would be expected since the wall temperatures there are the lowest. The maximum intensity is at the center of the furnace because there the view factors and furnace temperature are largest. The intensity at the top of the furnace is approximately 75 per cent of the maximum. To account for these variations in radiation intensity on the absorptance of the aerosols investigated it will be necessary to compute the residence time of the aerosol as a function of position within the furnace and to integrate the exposure rate along the furnace to yield a total exposure.

---

(2) R. B. Bird, W. E. Stewart, and E. N. Lightfoot, Transport Phenomena, John Wiley and Sons, Inc., New York, 1960, p. 409.

IV. ANALYSIS

A. Experimental Precision and Reproducibility

The results presented in this report have varying precision limits since many of the experiments were performed to develop a procedure that would yield the best possible results with the existing equipment. In this regard intensive effort was devoted to the accurate assessment of the energy absorbed by the calorimeter coolant for a basic and readily apparent error was incurred in this determination. Initially there was an uncertainty of about ± 3.0 Btu/min when water was the coolant. Later measurements were much improved; air serving as the calorimeter coolant reduced the uncertainty to ± 0.1 Btu/min.

Additional variations resulted from the adhesion of particles to the quartz conduit wall, thus changing the effective intensity of the radiant field. It is believed that this phenomena was the basic factor in the unaccountable variations in the experimental results, which at times ranged as high as ± 0.5 Btu/min and constituted the principal experimental uncertainty. Certain other factors affected the operation, but, over the time interval of a complete run, were established by experimental observation to have only a small net effect. Such factors included the powder flow rate, furnace temperature and air flow rate. These latter variables were under constant surveilance to insure operational stability.

Prevailing fluctuations in the furnace temperature and the air flow rate did not produce significant variations in experimental measurements. Instantaneous changes in the powder flow rate, on the other hand, gave readily detectable effects. Figure 11 shows the

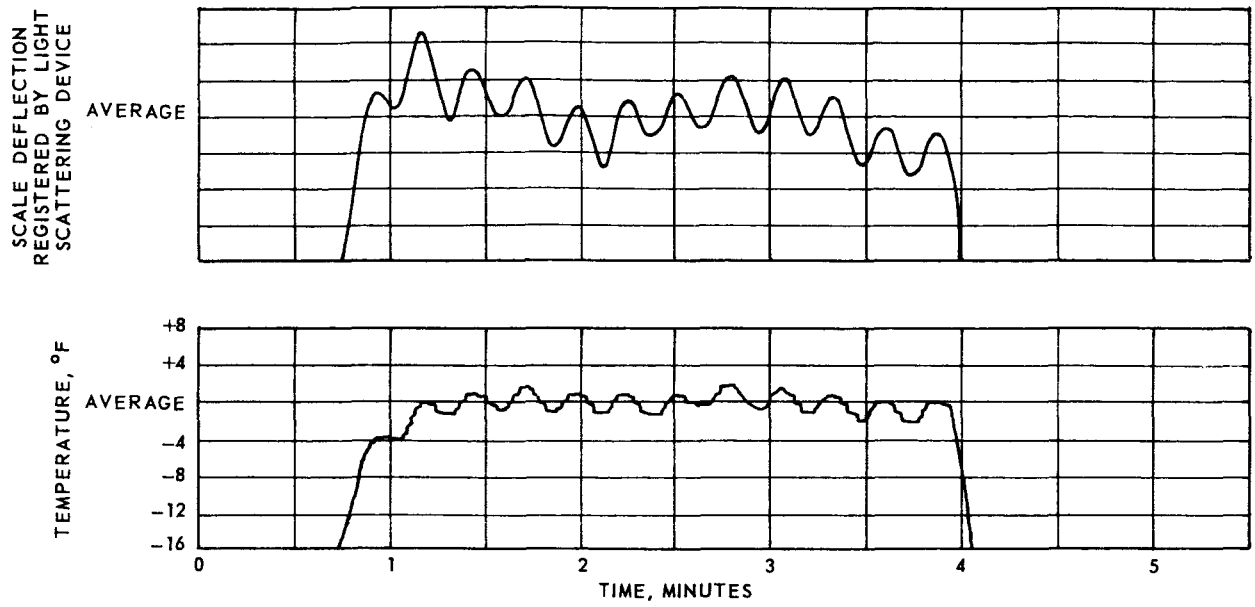

1. FeS 0.025 AVERAGE PERCENT BY VOLUME AT 70°F AND 1 ATM. (0.24 LB/MIN)

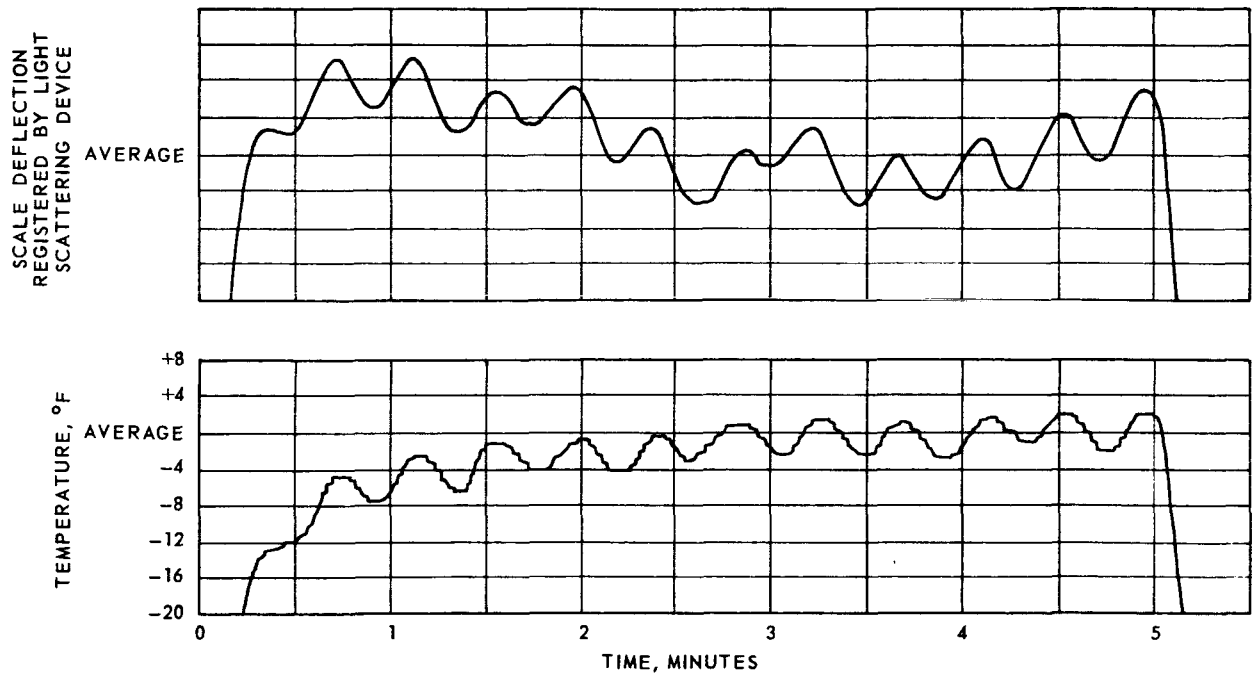

2. FeS 0.017 AVERAGE PERCENT BY VOLUME AT 70°F AND 1 ATM. (0.16 LB/MIN)

Figure 11. The Variation of Powder Concentration as Indicated by Light Scattering Device and the Corresponding Fluctuations of Aerosol Temperature Measured at Exit of Calorimeter.

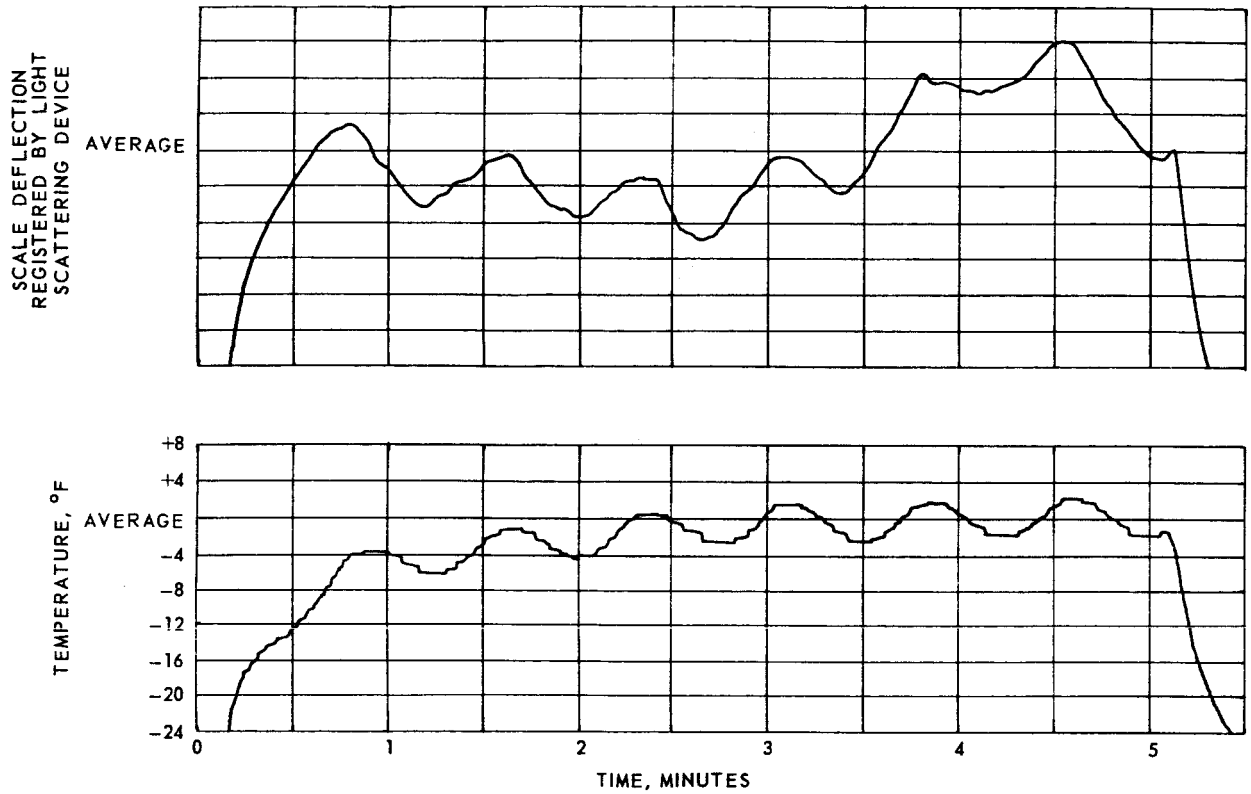

3. FeS 0.092 AVERAGE PERCENT BY VOLUME AT 70°F AND 1 ATM. (0.089 LB/MIN)

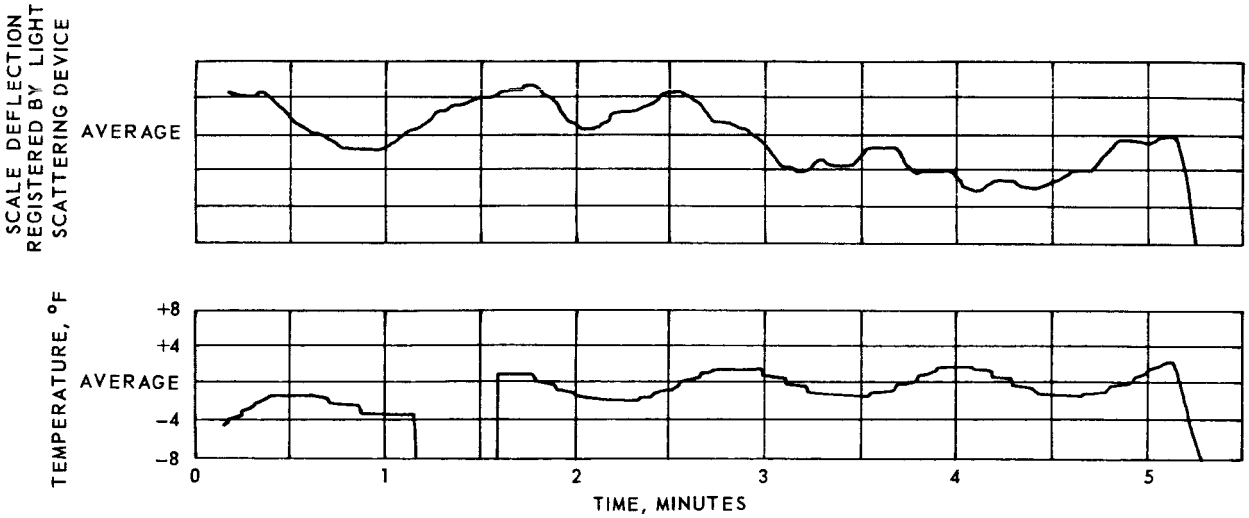

4. FeS 0.061 AVERAGE PERCENT BY VOLUME AT 70°F AND 1 ATM. (0.059 LB/MIN)

Figure 11 (Continued). The Variation of Powder Concentration as Indicated by Light Scattering Device and the Corresponding Fluctuations of Aerosol Temperature Measured at Exit of Calorimeter.

variation of concentration with time and the resulting particle-cloud temperatures measured at the exit from the calorimeter. The variation in concentration represented is not known exactly, although it appears to be within about 2 per cent. Direct sampling showed that the maximum variation over an extended time interval never exceeded ± 5 per cent. The amplitudes of the temperature changes are shown in Figure 11. The periodic fluctuations were caused by the rotation mechanism within the aerosol generator, and were of different frequencies for each level of powder concentration since the powder output was changed by variation of the aerosol generator speed.

B. Heat Absorbed by Particle Cloud Systems

Heat can enter the particle cloud system by four processes: (1) radiation to the particles, (2) radiation to the glass conduit conveying the aerosol, (3) conduction and convection at the end of the quartz conduit where it is not protected by a vacuum jacket, and (4) radiation to particles adhering to the quartz walls in the furnace. Except for the heat absorbed by the particle cloud, the heat gained by the particle-gas system was nearly constant at 10 Btu/min and was principally due to radiation absorbed by the glass. Heat conveyed to the system by end effects was not determined though it was held to a minimum by protecting the ends as much as possible from radiation and from surrounding high temperature gases. To show that end effects were not major factors, a temperature distribution along the quartz tube was made. As shown in Figure 12 there was not a significant discontinuity in the gas temperature near the ends. The constantly rising temperature shown was due to radiation received by the glass.

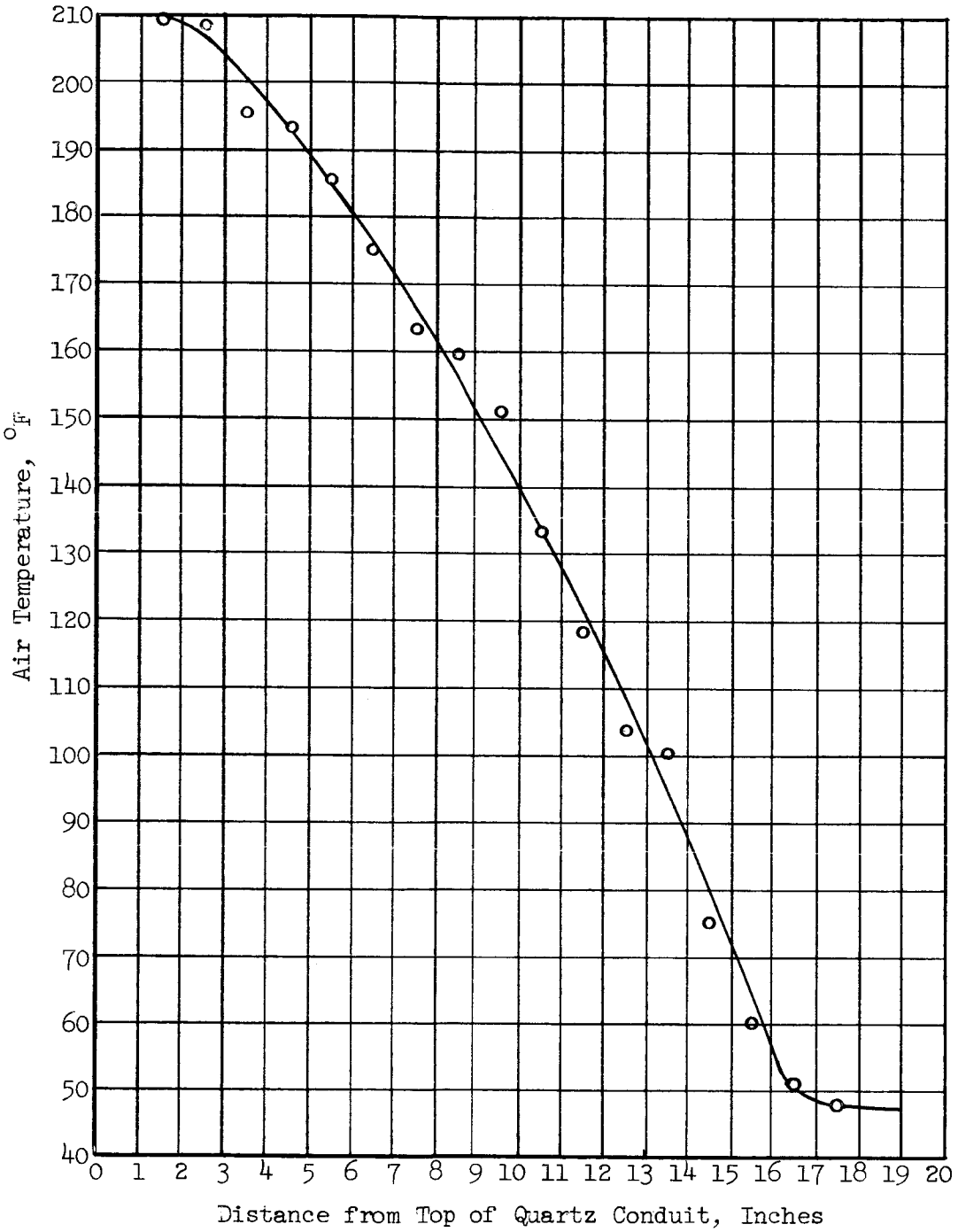

Figure 12. Temperature Profile in Heated Portion of Quartz Conduit

Such were the conditions under which the absorptance of particle-clouds have been measured. It would be desired to have no heat gain by the system other than from absorption by the cloud. This, however, cannot be achieved since any quartz wall, however thin, would absorb radiation to some extent and there would always be some absorbing particles adhering to the wall. The effect of the ideal system, nevertheless, can be calculated from the data on the present system.

Figure 13 presents the theoretical temperature rise that would occur in the particle-gas systems, if they were receiving radiant absorptance from the particles only. Thus,

$$\Delta t = \frac{Q_{abs}}{(MC_p)_{parts} + (MC_p)_{air}}$$

It may be noted that although the cloud absorptance may be essentially linearly dependent on particle concentration (for example, see Figure 10), the temperature rise as a function of concentration is nonlinear and approaches the asymptotic value $\frac{Q_{abs}}{(MC_p)_{parts}}$. This ultimate temperature rise cannot be attained physically, however, because particle shading would, for any powder, retard the linear dependence of heat absorbed on concentration. The concept, nevertheless, is useful in evaluating the ability of an aerosol to heat itself by the absorption of radiation. For the curves in Figure 13, the aysmptotic values are 300° F for the 30 - 44 micron ferrous sulfide, 118° F for the 44 - 53 micron ferrous sulfide, 178° F for zinc and 78° F for the 53 - 88 micron ferrous sulfide. The temperature rise can be made larger only by increasing Q_{abs} which, in turn, is a function of furnace temperature, particle size, material,

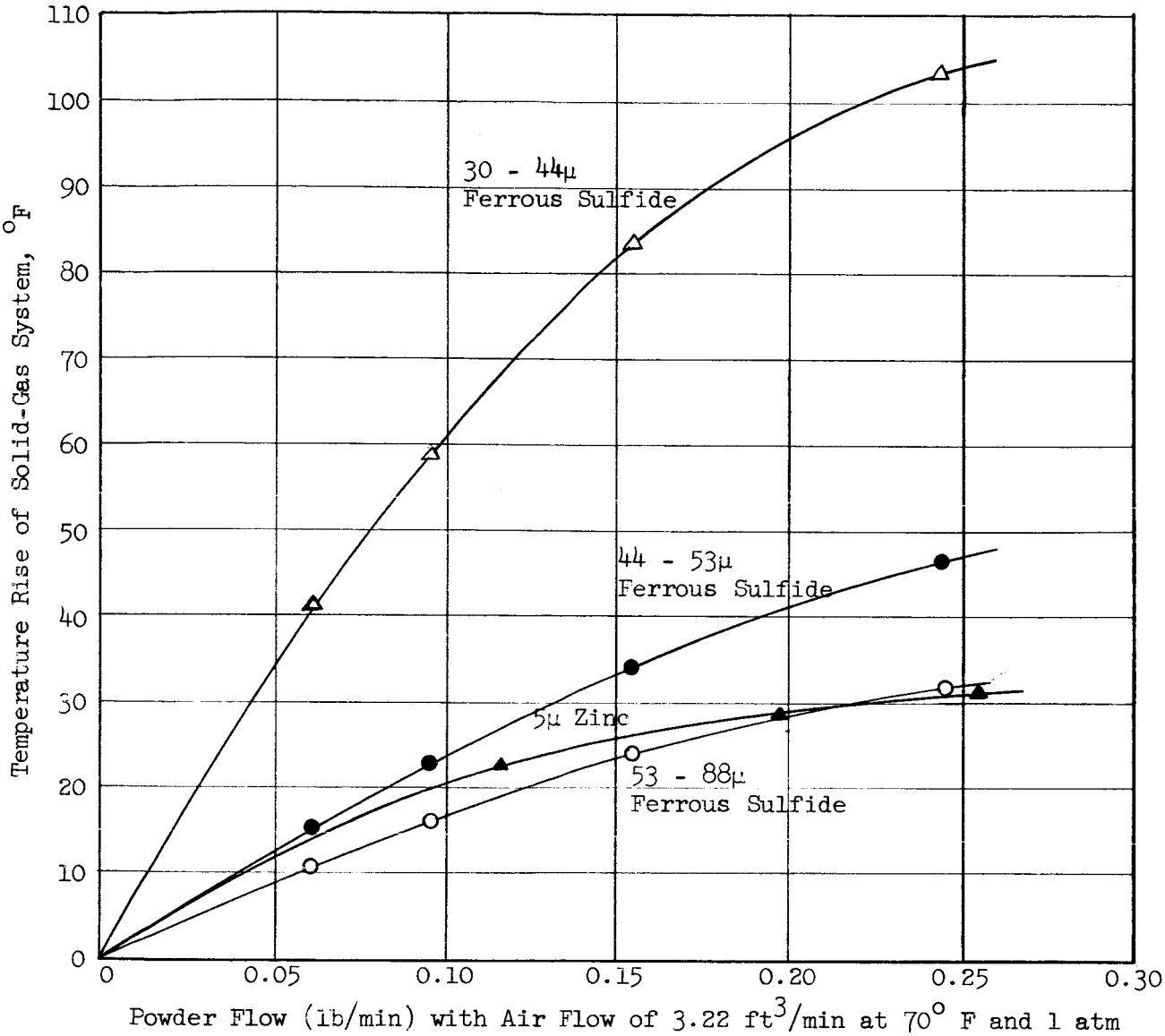

Figure 13. Calculated Temperature Rise of Aerosol Due to Particle Absorption Alone

and concentration. Higher source temperatures increase the radiant flux and hence the absorptance. Decreasing particle size increases the absorptance as long as the particles are large enough to remain opaque, and radiation scattering does not become dominant in the particle radiation extinction coefficient; thereafter the absorptance can decrease (an analysis of this variable is presently in progress). Increasing the particle concentration raises the absorptance until particle shading becomes dominant; then, the absorptance may rise further or remain essentially constant, depending on the size and reflective properties of the particles and on the geometry of the system. As shown in Figure 9 the absorptance of ferrous sulfide aerosols increased throughout the concentration range studied. The zinc particle clouds (Figure 8) were reaching a maximum at the upper concentration levels.

C. Significance of Data

Two major results are expected to be derived from the present developments. One is the prediction and experimental verification of the absorptivity of a particle cloud and the second is a description of the rate of heat dissipation and the associated surrounding temperature profiles for particles being heated by radiation. With respect to the former objective, particle radiation properties are extremely complicated functions of material, size, shape, surface properties, and radiation source; the exact treatment is not feasible due to the irregularity in shape and size of the particle comprising the cloud. The approach, then, is to measure certain particle dimensions so that the average for a large number of particles would be descriptive for radiation calculations. A theoretical development of this type is

presently being pursued to treat the particles as cylinders so that the irregularity of the particles, at least to some degree, can be considered.

According to the Mie theory and calculations by Van de Hulst (3), there are three domains of particle dimensions and radiation wave lengths to be considered. These domains are expressed as ratios of particle diameter to radiation wave length: ratios less than one, approximately one, and greater than one. Presently, the greater-than-one domain is being considered, the particles ranging in diameter from 100 to 5 microns. Future work will consider particles smaller than 5 microns. The thermal radiation of the present furnace is predominately in the 1 to 3 micron range; hence, the particles are considerably larger than the wave length. Indications are that situations of this type can be treated reasonably accurately by the ordinary laws of optics. It is being attempted, therefore, to employ these principles together with an assumed particle geometry and transmissivity constant to develop a correlation for particles larger than the wave length of the impinging radiation.

The utility of this approach is that the correlations derived here will be applicable to other systems where smaller particles and higher temperatures are employed, a condition more likely to be encountered in practical problems involving radiation. For higher temperatures on the order of $50,000^{\circ}$ R, the peak radiation intensity is at a wave length of 0.1 micron and most of the radiation is less than 0.2 micron. Thus, particles of sizes as low as about one micron

---

(3) H. C. Van De Hulst, Light Scattering by Small Particles, John Wiley and Sons, Inc., New York, 1957.

$\left(\frac{d}{\lambda} \geq 5 \right)$ exposed to this radiation experience effects similar to those presently being studied. Moreover, small particles, which are not good electrical conductors, are to a large extent transparent, a condition also being included in this investigation. Because of the deagglomeration problems of the smaller particles and the inaccessibility of the higher temperature in an experimental apparatus, it is impractical to obtain data, particularly reliable data, for the more exotic systems. The analogous systems being studied, however, can be readily deagglomerated and more reliably investigated.

Approximate numerical solutions have been presented previously (4) for predicting the particle and associated surrounding air temperature profiles for particles being heated by radiation. Due to the approximate nature of the solutions and the difficulty of applying them to the present investigation, a simpler approach has been undertaken. This analysis assumes quasi-steady state behavior and yields closed form solutions for both the particle and surrounding average air temperatures as functions of the pertinent system parameters. These results are for the case of all heat transfer being by radiation to the particles and then by conduction from the particles to the gas. Charts have been prepared for this case. It was hoped that the case analyzed would be applicable to the experimental system. However, as discussed previously, experiments indicated that an appreciable fraction of the energy transferred to the gas-particle system was by convection from the wall of the confining tube. Consequently, the analysis is being extended to apply to the actual case. All of these results will be presented later.

---

(4) A. McAlister, H. C. Ward, C. Orr, Jr., Heat Transfer to a Gas Containing a Cloud of Particles, Semiannual Status Report No. 2, Project No. A-635, Engineering Experiment Station of the Georgia Institute of Technology, Atlanta, Georgia, June 15, 1963, 35 pages.

V. FUTURE WORK

Future experimental work will extend the collection of data to include a spectrum of powders having different absorption characteristics. Particular attention will be given to selecting materials of varying absorption thicknesses. These data will be employed, together with theoretical results, to study the absorptive properties of particles having a significant part of their volume penetrated by radiation.

The theoretical work presently in progress will be continued. This will include calculations for the absorption of particles taken as cylinders and extension of the quasi-steady-state analysis for particles and associated average air temperatures for the case where both radiation and convection heat transfer mechanisms are important.

Respectfully submitted

Clyde Orr, Jr.

Clyde Orr, Jr.
Project Director

Approved:

Frederick Bellinger,

Frederick Bellinger, Chief
Chemical Sciences and Materials Division